Diving behavior of Cuvier's beaked whales inferred from 3D acoustic localization and tracking using a nested array of drifting hydrophone recorders

Jay Barlow[a)]
NOAA National Marine Fisheries Service, Southwest Fisheries Science Center, Marine Mammal and Turtle Division, 8901 La Jolla Shores Drive, La Jolla, California 92037, USA

Emily T. Griffiths[b)]
Ocean Associates, Inc., 4007 North Arlington Street, Arlington, Virginia 22207, USA

Holger Klinck
Bioacoustics research Program, Cornell Laboratory of Ornithology, Cornell University, 159 Sapsucker Woods Road, Ithaca, New York 14850, USA

Danielle Harris
Centre for Research into Ecological and Environmental Modelling, The Observatory, Buchanan Gardens, University of St. Andrews, St. Andrews, Fife, KY16 9LZ, United Kingdom.

Date uploaded: 1 August 2018
Running title: 3D dive tracking for beaked whales

Echolocation pulses from Cuvier's beaked whales are used to track their three-dimensional diving behavior in the Catalina Basin, California. In 2016, five two-element vertical hydrophone arrays were suspended from the surface and drifted at ~100-m depth. Cuvier's beaked whale pulses were identified, and vertical declination angles were estimated from time-differences-of-arrival of either direct-path signals received on two hydrophones or direct-path and surface-reflected signals received on the same hydrophone. A Bayesian state-space model is developed to track the diving behavior. The model is fit to these detection angle estimates from at least four of the drifting vertical arrays. Results show that the beaked whales were producing echolocation pulses and are presumed to be foraging at a mean depth of 967 m (s.d. = 112 m), approximately 300 m above the bottom in this basin. Some whales spent at least some time at or near the bottom. Average swim speed was 1.2 m s^{-1}, but swim direction varied during a dive. The average net horizontal speed was 0.6 m s^{-1}. Results are similar to those obtained from previous tagging studies of this species. These methods may allow expansion of dive studies to other whale species that are difficult to tag.

[a] Electronic mail: jay.barlow@noaa.gov

[b] Also at: NOAA National Marine Fisheries Service, Marine Mammal and Turtle Division, Southwest Fisheries Science Center, 8901 La Jolla Shores Drive, La Jolla, California 92037, USA

I. INTRODUCTION

The detailed diving behavior of most whales is not directly observable by humans. Diving studies are especially challenging for deep-diving whales such as beaked whales (family Ziphiidae), for which each foraging dive can last more than two hours at depths of up to 3,000 m (Schorr et al. 2014). Most of what we currently know about beaked whale diving behavior comes from tagging studies. Time-depth recorders have been used to quantify dive times and depths, inter-dive periods, and descent and ascent rates (Tyack et al. 2006; Baird et al. 2008). Acoustic recording tags have added the ability to study details related to their foraging behavior (Johnson et al. 2004; Tyack et al. 2006). Multi-sensor tags that also include accelerometers and magnetic headings allow even more detailed re-constructions of three-dimensional (3D) diving and foraging behavior (Johnson et al. 2008; Laplanche et al. 2015). However, tagging studies have been successfully applied to only a small subset of the 22 species of beaked whale.

One of the better studied species is Cuvier's beaked whale (*Ziphius cavirostris*) which have been tagged in the Mediterranean (Johnson et al. 2004; Tyack et al. 2006), Hawaii (Baird et al. 2008), Southern California (DeRuiter et al. 2013; Schorr et al. 2014) and the Azores (F. Visser, pers. comm.). In general, diving behaviors were similar in different areas. To summarize from those studies, Cuvier's beaked whales typically conduct deep foraging dives with mean durations of 60-70 minutes and with mean inter-deep-dive periods of 60-100 minutes. During a deep foraging dive, whales descend at a rate of ~1.4-1.5 m s^{-1} to a depth of ~450 m before initiating echolocation and foraging. Whales forage typically for ~35 min at depths of 700-2,000 m (and as deep as 3,000 m) before returning to the surface. During their ascent, whales stop echolocation at a depth of ~850 m and continue to ascend at a slower rate (0.6-0.7 m s^{-1}) than their descent. During inter-deep-dive periods, whales make several shorter (15-21 min) dives to shallower depths and surface multiple times during relatively short (~2-3 min) surfacing series. The only other extensively tagged beaked whale species, Blainville's beaked whale (*Mesoplodon densirostris*), shows very similar behavior but generally has shorter foraging dives to shallower depths (Tyack et al. 2006; Baird et al. 2008).

Because beaked whales make regular echolocation pulses during foraging dives (Johnson et al. 2004; Zimmer et al. 2008), passive acoustic tracking is an alternative tool to study their diving behavior. To date, this approach has been largely limited to studies of sperm whales (*Physeter macrocephalus)*. Large-aperture arrays of bottom-mounted, surface-suspended or towed hydrophones have been used to determine the 3D diving behavior of vocalizing sperm whales (Møhl et al 2000; Thode 2004; Nosal and Frazer 2007; Miller and Dawson 2009; Baggenstoss 2011). A key element to these studies is the localization of their echolocation pulses using time-difference-of-arrival (TDOA) of the sounds on multiple hydrophones. At sea, cabled hydrophone arrays are unwieldy at scales greater than a few hundred meters, so multiple autonomous recorders are often used to create larger aperture arrays. Maintaining recording synchrony is problematic for autonomous recorders because digital clocks with sufficient precision to accurately measure TDOA are not widely available in commercial recording systems. Several clever approaches have been developed to establish recording synchrony and

thereby accurately measure TDOA from widely separated hydrophones. Møhl et al. (2000), McGehee (2000), and Wahlberg et al. (2001) developed methods that used radio-linked hydrophones to record simultaneous signals on a single recorder. Møhl et al. (2001) and Miller and Dawson (2009) used precise GPS timing signals recorded synchronously with the audio recordings from each independent hydrophone to establish a precise time reference. Thode (2004) used two widely spaced elements in linear array and used surface reflections to effectively simulate a large spatial array. Baggenstoss (2011) developed TDOA methods to simultaneously localize multiple individuals. Gassmann et al (2013) described a system for 3D tracking of another species, killer whale (*Orcinus orca*), using a series of several cabled hydrophone arrays suspended from a floating platform.

In many ways, sperm whales are a model species for localization studies. Sperm whales produce loud echolocation clicks with source levels up to 223 dB re: 1 uPa RMS @ 1 m (Møhl et al. 2000), and even though their clicks are highly directional (Møhl et al. 2000), off-axis signals can be discerned at ranges of several kilometers (Nosal and Frazer 2007; Miller and Dawson 2009). Inter-click-intervals are stable and relatively long for sperm whales, which facilitates localization of individuals within groups. Also, their deep-diving behavior makes it difficult to study this species from surface observations alone, which increases the value of passive acoustic methods.

Beaked whales of the family *Ziphiidae* are also hard-to-study, deep-diving whales, but aspects of their biology and behavior limit the application of the same approaches. Beaked whale echolocation pulses are much higher in frequency (10-90 kHz, Baumann-Pickering et al. 2013) than those of sperm whales (0.1-20 kHz, Nosal and Frazer 2007), which prevents the use of off-the-shelf radio equipment to transmit their audio signals to a central recording system. More significantly, the echolocation pulses of the best studied species of beaked whale (Cuvier's beaked whale and Blainville's beaked whale) are highly directional and with an estimated -3 dB beam widths of only 6° (Zimmer et al. 2008). Off-axis echolocation signals of Cuvier's beaked whale are estimated to be detectable above ambient noise only to a distance of ~700 m (Zimmer et al. 2008). Given that the typical foraging depths of this species is greater than 700 m, only on-axis pulses are likely be detectable on near-surface hydrophones. Studies with large-aperture arrays of bottom-mounted arrays have shown that, due to their narrow beam widths, on-axis pulses are seldom likely to be received simultaneously on a sufficient number of hydrophones to allow localization (Ward et al. 2008).

Several approaches have been developed for 3D acoustic tracking that do not rely on the same signal being received on a widely distributed array of time-synchronized hydrophones. Gassmann et al. (2015) used a nested array configuration with two small-aperture, four-element arrays (nodes) nested within a large-aperture array of single-channel recorders for 3D tracking of Cuvier's beaked whales. Each small-aperture array is used to estimate the direction to a sound source in three dimensions, and each hydrophone is recorded on the same instrument, so timing synchrony was not an issue. Although Gassmann et al. (2015) established recording synchrony of widely spaced elements by measuring and adjusting for clock drift, his nested method also

allows for localization without precise synchronization between recorders. This approach can work even when the same signal is not received at both nodes, so long as signals from the same whale are received by both nodes within a time period that is short enough that animal movement is negligible. DeAngelis et al. (2017) used bearing angles from a towed hydrophone array, target motion analysis, and reflected angles to localize several species of beaked whale in the Atlantic. For sperm whales, Nosal and Frazer (2007) avoided the need for precisely synchronized recordings in 3D tracking by utilizing both direct-path and surface-reflected signals received on at least four seafloor hydrophones to localize based on signals received within a 20-sec time interval. Methods such as these that do not require the same signal to be received on widely spaced hydrophones and do not require precise time synchronization are ideal for passive acoustic tracking of beaked whales.

Here we present a passive acoustic approach to tracking the 3D diving behavior of whales using a spatial array of unsynchronized hydrophone recorders suspended under drifting buoys. Each node of this large-aperture array is comprised of a vertical array of two closely-spaced (10 m), near-surface hydrophones recorded in stereo. TDOA of echolocation pulses on the vertical arrays are used to estimate declination angles. We test this nested array configuration of a large aperture, unsynchronized spatial array comprised of time-synchronized vertical arrays to study diving behavior of Cuvier's beaked whales in the Catalina Basin, California during 2-weeks in July and August 2016. Although the same echolocation pulse is seldom received on more than two nodes, pulses are often received on 3-5 nodes within a relatively short time snapshot, allowing precise localization. We develop a discrete-time, state-space model to track whales using a movement model that constrains travel speed to biologically feasible values and a measurement model that uses the declination angles from multiple vertical arrays. Occasionally available surface reflections provide independent measurements of declination angles and allow correction for small degrees of array tilt. Aspects of diving behavior are inferred from ten estimated 3D dive tracks.

II. METHODS

We use declination angles measured from a drifting array of hydrophones at ~100-m depth for both localization and tracking of Cuvier's beaked whales. In this paper, we use the term localization to refer to the estimation of a 3D location (in planar space and depth) at a single point in time. As we use this term, localization does not use information from previous or subsequent locations. We use the term tracking to refer to a time series of 3D locations that are estimated in a model. Within the context of the model, estimates of tracking locations are influenced by previous and past locations and can be constrained to realistic values by parameters in the model. Declination angles to the source of a beaked whale echolocation pulse are estimated using two methods: A) the TDOA of a pulse on two elements of a vertical hydrophone array and B) the TDOA of a pulse and its surface reflection on a single hydrophone. Method A provides an estimate of declination angle from the mid-point of the two elements and

is subject to error from array tilt relative to the source; this method is only used in tracking. Method B (often referred to as a virtual array, Cato 1998) provides an estimate of declination angle from the surface and is not affected by array tilt; this method is used in both localization and tracking.

A. Localization

Localization of a beaked whale in three dimensions at a single point in time is achieved using the TDOA between direct-path and surface-reflected echolocation pulses (method B) received at a minimum of three locations within a short (2-min) time window. Downward conical bearing angles from four points on the sea surface converge exactly at only one point; however, angles from three locations converge at two points and can sometimes provide unambiguous localization if one of those points is implausible (deeper than the seafloor or shallower than the foraging depths of beaked whales). Exact convergence is not guaranteed given measurement error, so we use a maximum likelihood (least-squares) approach to find the best-fit point-of-convergence. Latitude (Y) and longitude (X) are expressed in kilometers using the Universal Transverse Mercator (UTM) coordinate system. At a beaked whale's horizontal location (X, Y), the depth of a point on a downward-opening cone, j, can be estimated from the location of its apex at the sea surface (x_j , y_j) and the conical angle, β_j. For β_j conical angles at j locations, predicted depths, Z_j at (X, Y) can be estimated as

$$Z_j = R_j * tan(\beta_j) , \quad (1)$$

where R_j , the horizontal range of (X, Y) from apex j, is estimated as

$$R_j = \sqrt{\left(X - x_j\right)^2 + \left(Y - y_j\right)^2}. \quad (2)$$

The R (R Core Team 2013) function *optim* is used to find the position (X, Y) that minimizes the sum of squared deviations in the estimated and mean ranges (linear fitting methods would work as well)

$$\sum_j (R_j - \sum \frac{R_j}{n})^2 . \quad (3)$$

We estimate the location of beaked whales using angles estimated only from reflected signals because the measurement of these is not affected by array tilt. We assume that animal movement is small within the 2-min interval used for localizations (see Discussion) and ignore a trivially small correction for curvature of the earth.

B. Tracking

Beaked whale 3D dive tracks are reconstructed using detection angles estimated from at least four DASBRs. Locations in time and space are modeled using a hidden-Markov, state-space model (MacDonald and Zucchini 1997) in a Bayesian framework. Locations are treated as a latent state constrained by an animal movement model that imposes biological feasibility constraints. Detection angles are used in a measurements model. The model is parameterized with discrete time steps of one minute (Δt).

Location in space is assumed to be a Markov function of the previous location and velocity vectors. Here we use X as longitude and Y as latitude (again in UTM meters) and Z as depth in meters, and X', Y', and Z' as corresponding velocities. Location at time $i+1$ can be specified as

$$X_{i+1} = X_i + X'_i \cdot \Delta t \quad (4)$$

$$Y_{i+1} = Y_i + Y'_i \cdot \Delta t \quad (5)$$

$$Z_{i+1} = Z_i + Z'_i \cdot \Delta t \ . \quad (6)$$

Velocities are specified by an animal movement model that is based on x-y (horizontal) heading (H), vertical pitch (P), and speed through the water (S).

$$X'_{i+1} = S_{i+1} \cdot \sin(P_{i+1}) \cdot \cos(H_{i+1}) \quad (7)$$

$$Y'_{i+1} = S_{i+1} \cdot \sin(P_{i+1}) \cdot \sin(H_{i+1}) \quad (8)$$

$$Z'_{i+1} = S_{i+1} \cdot \cos(P_{i+1}) \ . \quad (9)$$

Heading, pitch, and speed are estimated from previous values plus normally distributed random deviations (δ) with zero means and standard deviations taken from broad uniform distributions.

$$H_{i+1} = H_i + \delta_H \ ; \ \delta_H \sim N(mean=0, sd=\sigma_H); \ \sigma_H \sim U(0.05, 1.0); \text{ in radians} \quad (10)$$

$$P_{i+1} = P_i + \delta_P \ ; \ \delta_P \sim N(mean=0, sd=\sigma_P); \ \sigma_P \sim U(0.0, 1.5); \text{ in radians} \quad (11)$$

$$S_{i+1} = S_i + \delta_S; \ \delta_S \sim N(mean=0, sd=\sigma_S); \ \sigma_S \sim U(0.1, 0.5); \text{ in m s}^{-1} \quad (12)$$

The state variables are estimated by minimizing the deviations between the observed detection angles for each DASBR and the expected detection angles given the DASBR locations and the state variables. Expected ranges ($R_{i,j}$) at each time step i to each DASBR j are estimated as the square root of the sum of squared differences in UTM values of easting and northing (Eq. 2). Predicted detection angles for direct-path ($\alpha_{i,j}$) and reflected-path ($\beta_{i,j}$) angles were estimated from these range estimates, animal depth estimates (Z_i), and the mean hydrophone depth of each DASBR ($D_{i,j}$).

$$\alpha_{i,j} = \operatorname{atan}(R_{i,j} / (Z_i - D_{i,j})) \quad (13)$$

$$\beta_{i,j} = atan(R_{i,j} / Z_i) . \quad (14)$$

Predicted angles are modeled as the sum of observed angles ($O_{i,j}$), normally distributed random errors (ε) with zero mean, and, for direct-path angles, a DASBR-specific correction for array tilt (T_j).

$$\alpha_{i,j} = O_{i,j} + T_j + \varepsilon_{\alpha j} ; \ \varepsilon_{\alpha j} \sim N(mean=0°; sd=0.80°) \quad (15)$$

$$\beta_{i,j} = O_{i,j} + \varepsilon_{\beta j} ; \ \varepsilon_{\beta j} \sim N(mean=0°; sd=0.10°) . \quad (16)$$

Array tilt does not affect angles β estimated from surface reflections, so array tilt is assumed to be zero for these angles. In this model, ε values represent measurement error and T values represent bias in the direct-path angles. The standard deviations for ε_α and ε_β are based on a previously measured value for direct-path and reflected angles for DASBRs (sd = 0.80° and 0.10°, respectively, Barlow and Griffiths 2017). The prior distribution for the array tilt correction is modeled as a broad normal distribution with a mean of zero and a standard deviation of 5°.

$$T_j \sim N(mean=0°; sd=5.0°) . \quad (17)$$

The Bayesian posterior distributions of estimated location and other variables are estimated using Markov Chain Monte Carlo (MCMC) algorithms as implemented in OpenBUGS software (Lunn et al. 2009). A short description of this software, alternative methods for fitting state-space models, and the OpenBUGS code for this model are available in supplemental material[1]. OpenBUGS software is accessed using the *R2OpenBUGS* package v3.2 in R v3.4.2. Estimated parameters include the initial states (X_1, Y_1, Z_1, H_1, P_1, S_1), the standard deviations of the normally distributed, zero-mean terms (σ_H, σ_P, and σ_S), and the DASBR-specific values of the deviations in heading, pitch and speed between each time step in the model (δ_H, δ_P, and δ_S). Non-informative uniform distributions (Lunn et al. 2012) were used for initial speed, pitch and heading (H_1, P_1, S_1). To improve convergence, a plausible initial location (X_1, Y_1, Z_1) was determined by trial and error, and this initial location was specified as a normally distributed prior with a standard deviation of 1 km horizontally and 0.3 km vertically. Speeds (S_i) are constrained to biologically plausible values (0.25 to 3.5 m s^{-1}). Posterior probabilities were based on 200,000 iterations with a thinning ratio of 1:100 after a burn-in of 200,000 iterations (see Lunn et al. 2012 for an explanation of these parameters in OpenBugs).

C. Array design

Cuvier's beaked whales were localized and tracked using a nested array design comprised of a large aperture array of four to eight drifting nodes. Each node is comprised of a two-element vertical array with hydrophones separated by 10 m and a two-channel autonomous digital recorder (see Figure 2 in Griffiths and Barlow 2015). The nodes were deployed initially

in two north-south rows with ~900 m separation between rows and between nodes within each row (Fig. 1); however, this array geometry changed during each drift due to random effects of current and wind. Three of our eight recorders failed to record useable data, largely due to problems with underwater connectors, so results presented here will be from arrays with four or five nodes.

FIG. 1. Drifts of buoy recorders in the Catalina Basin (white lines). Eight buoys were typically deployed in a 2 x 4 rectangular configuration separated by ~ 900 m (as exemplified by black and white circle symbols) and drifted northeast. Black and white square symbols indicate localized Cuvier's beaked whales (Table I). Drifts were designed to pass over two seafloor recorders (triangles) as part of a different study.

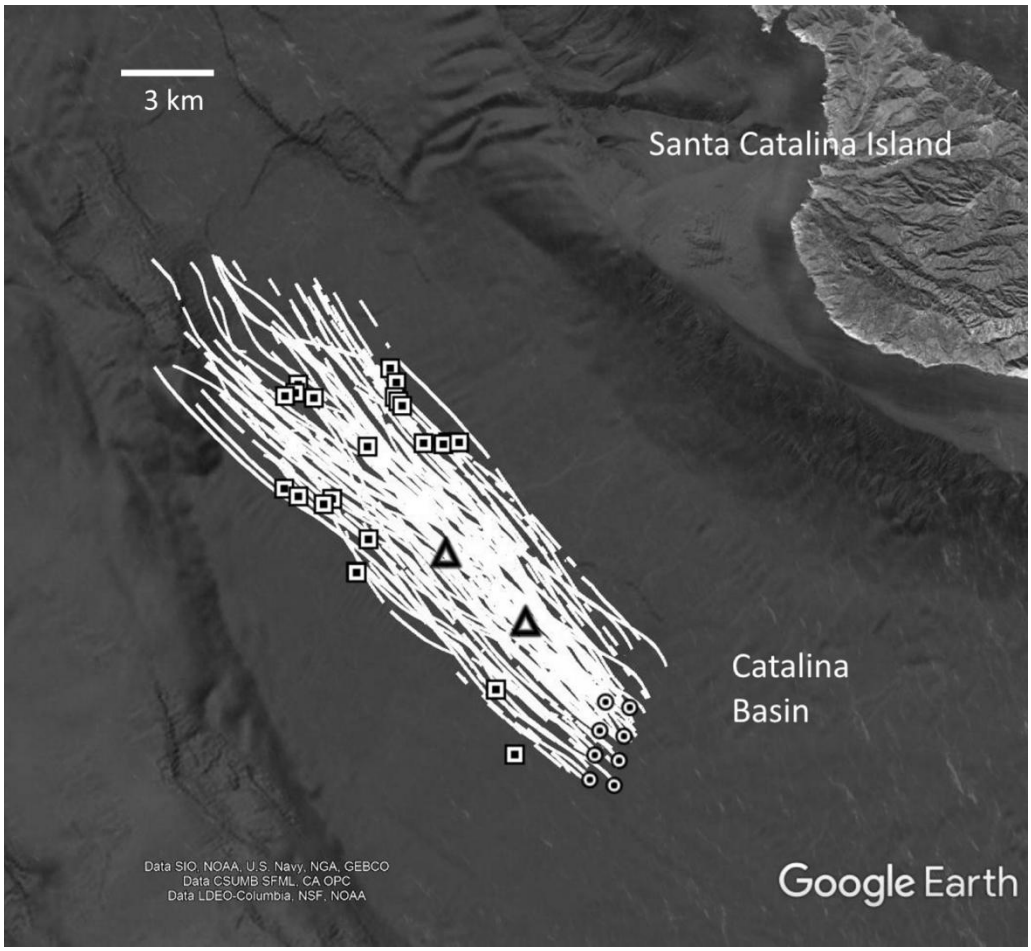

One of the five functioning nodes (designated W-4) was based on the Griffiths and Barlow (2015; 2016) design for a drifting acoustic spar buoy recorder (DASBR v1). It used a Wildlife Acoustics SM2+Bat recorder mounted in a PVC spar buoy. Stereo acoustic files were recorded continuously in 5-minute WAV-format files at a 192 kHz sample rate. A Kevlar-reinforced underwater Cat-5 cable (Falmat FMXCAT50000K12) connected two hydrophones (at ~90 m and ~100 m depths) to the floating instrument package. The hydrophones (High Tech, Inc. HTI-96-min) had a sensitivity of -182 dB re:1V/µPa and a useable frequency range from 50

Hz to 140 kHz. A differential amplifier in the array added 34 dB of gain. Voltages from a pressure transducer near the hydrophones were recorded by the SM2+Bat recorder to measure depth. A 30-m x 8-mm elastic cord was attached to the conducting cable to decouple the movement of the surface buoy from the hydrophones. The SM2+Bat signal conditioning settings were zero gain on both channels, a 3 Hz high-pass filter on Channel 0 (upper hydrophone) and a 180 Hz high-pass filter on Channel 1 (lower hydrophone).

The other four functioning nodes (designated B-1 to B-4) used Wildlife Acoustics SM3M autonomous underwater recorders. This configuration (DASBR v2) differed from the previous design in using submersible recorders and a nylon line rather than a near-surface SM2+Bat recorder and a conducting cable. The record duty cycle for the SM3M recorders included a 1-min stereo WAV file at the top of the hour at 96kHz (for quiet ocean noise measurements), a 5-min sleep period (to force the system clock to synchronize with the temperature-compensated clock), and 27 2-minute WAV files at 256 kHz sampling rate. Two hydrophones (at ~105 m and ~115 m depths) were attached to a nylon line and were connected to the SM3M recorder with 10-m cables. The hydrophones (High Tech, Inc. HTI-96-min) had a sensitivity of -165 dB re:1V/µPa and a useable frequency range from 50 Hz to 140 kHz. A 30-m x 10 mm elastic cord was used immediately below the spar buoy to decouple the movement of the surface buoy from the hydrophones. A 50-m x 6-mm nylon line was used below the elastic cord, and the SM3M and hydrophones were mounted to a 15-m x 10-mm nylon line below that. The signal conditioning settings on the SM3M were 12 dB gain on both channels and a 2-Hz high-pass filter on both channels.

The overall configuration was similar for both the DASBR v1 and v2. Two Spot satellite geo-location devices (Gen3 and Trace models, used interchangeably) were mounted in the above-water section of the spar buoys to track and record GPS locations at intervals of 15-30 minutes. The vertical array orientation was maintained with a 6.5 kg weight at the bottom of each array.

D. Field studies

The array of DASBRs was deployed off southern California in the Catalina Basin from 19 July to 1 August 2016. Instruments were initially deployed from the San Diego-based 75-ft dive boat *Horizon*. The array was repositioned 12 times, typically on a daily basis, to re-establish the array geometry using the 25-ft research vessel *Vibrio* from the University of Southern California's Wrigley Marine Science Center. The drifts (Fig. 1) were designed to pass over two High Frequency Acoustic Recorders (HARPs) that were deployed on the seafloor as part of a separate study to compare beaked whale detections among instruments. The midpoint of all drifts was 33.2° N and 118.6° W. Four DASBRs (W-1 to W-4) were removed for data downloading and maintenance from 25-27 July. The other four (B-1 to B-4) were removed for data downloading and maintenance from 27 to 28 July.

E. Beaked whale identification and bearing angle estimation

Initial processing to identify beaked whale echolocation pulses and estimate direct-path vertical bearing angles used PAMGuard (Beta v1_15_03) open-source software[c] (Gillespie et al. 2008). Echolocation signals were detected using the PAMGuard energy-based click detector and were automatically classified by the PAMGuard click classifier into discrete categories based on peak frequency and the presence of a frequency upsweep (Keating and Barlow 2013). Direct-path, vertical bearing angles were automatically estimated within PAMGuard from the TDOA of the same echolocation pulse on the two elements of the vertical hydrophone arrays which were estimated by cross-correlation of the waveform data. The vast majority of echolocation signals in this area were from dolphins (especially common dolphins which were seen frequently during our field operations). Pulses that were likely to be from Cuvier's beaked whales were initially identified based on having a 22-24 kHz or 34-40 kHz peak frequency, at least occasional upsweeps as determined by the PAMGuard click classifier, and vertical bearing angles from below the array that were relatively consistent over several minutes. Consistent downward bearing angles were the most effective diagnostic for identifying beaked whale echolocation pulses in the presence of larger numbers of dolphin clicks. Characteristics of Cuvier's beaked whale pulses in this area have been described by Baumann-Pickering et al. (2014). Likely Cuvier's beaked whale detections were confirmed using four criteria: 1) presence of a clear upsweep in the Wigner plot of high SNR pulses, 2) presence of frequency peaks at 18, 22-24, and 34-40 kHz, 3) presence of a frequency valley or notch at 27 kHz, and 4) inter-pulse intervals greater than 250 msec. In some cases, context-specific information such as the presence of surface reflections and inter-pulse intervals were helpful in confirming species identification (Zimmer and Pavan 2008). Beaked whales were initially identified by independent analyses of all five DASBRs. If a beaked whale was confirmed on one or more DASBRs, data at that time from the remaining DASBRs were re-examined to determine whether a faint beaked whale may have been missed.

Surface-reflected signals from beaked whales are the sum of incoherent reflections off multiple wave faces, which reduces the precision of cross-correlation methods to estimate bearing angles. Therefore, the precise timing for surface-reflected signals was estimated using the Teager-Kaiser edge-detection approached developed by Barlow and Griffiths (2017). Vertical bearing angles for signals with strong surface reflections were estimated from the TDOA of direct-path and surface-reflected signals.

Estimated bearing angles were corrected for the expected sound speed profile for this month and area. The expected sound speed profile in the Catalina Basin in July at 49 discrete depths between 0 and 1,200m was estimated from temperature and salinity values in the U.S. Navy's Generalized Digital Environmental Model (GDEM-V, version 3.0.1; Carnes 2009) using the Mackenzie approximation implemented in the function *wasp* in the package *seewave* (Sueur

[c] https://www.pamguard.org/

et al. 2008) in R. Direct-path echolocation signals were initially processed in PAMGuard using a sound speed of 1,500 m s^{-1}, and estimated direct-path bearing angles were adjusted for the expected sound speed at 100 m (1490 m s^{-1}). The bearing angles for reflected signals were estimated based on the mean sound speed in the top 100 m of the water column (1,498 m s^{-1}). Bearing angle corrections for sound diffraction were estimated using the ray-tracing algorithm in the Matlab™ function *raytrace* (Val Schmidt, University of New Hampshire, 2009) based on a beaked whale at an assumed 1,000-m depth and at apparent detection angles from 10° to 80° from straight down. The ray-tracing algorithm used interpolated sound speed values at 1-m depth intervals based on a smoothing spline (from the R package *gam*) fit to the above sound speed data at 49 discrete depths. Corrections for diffraction ranged from a low of 0.04° at a detection angle of 10° to a high of 1.19° at 80°.

III. RESULTS

Individual DASBRs were deployed and retrieved 78 times during the 2-week project. The resulting drifts were towards the northwest and generally achieved the objective of drifting over the two seafloor recorders (Fig. 1). Average drift speeds were 0.76 km hr^{-1} (s.d. = 0.23 km hr^{-1}) and, given that the drifts were opposite the direction of the prevailing NW winds, were primarily driven by ocean currents. Twenty-nine dives of Cuvier's beaked whales were identified (see Table S1 in supplemental files[1]).

A. Localization

On 23 occasions during eleven of the 29 detected dives, unambiguous localizations could be calculated based on surface reflections received on at least three DASBRs within a 2-min time window (Table I). Localization was not possible for remaining 18 dives because surface reflections were not detected on at least three DASBRs within this time window. In some cases, two or three localizations were possible within a single dive. The mean estimated depths for these localizations is 977 m (sd = 171 m), and the estimated distances from the localization to the instruments range from 0.43 to 3.48 km (Table I).

B. Tracking

Eight of the eleven dives that had localizations were selected for tracking (Table II). In one of those eight dives (AI), tracks of three individuals were sufficiently distinct to allow each to be tracked separately, for a total of ten dive tracks (Table II). In three cases, dives were rejected from analysis because they represented groups of animals whose individual detection angles could not be unambiguously discriminated. Other dives were rejected because they did not have an unambiguous localization from surface reflections or were too short (less than 9

minutes). The sample includes dive segments from 9 to 32 min duration with an average of 21.4 min (Table II).

Illustrated results are provided for the longest tracked dive (AP-1). The detection angles for the five vertical hydrophone arrays (Fig. 2) steadily decline from the start until 27 min. elapsed time, indicating that the whale and the DASBR array were getting closer. This is also seen in the estimated track (Fig. 3A). At 27 min., the whale turns away from four of the vertical arrays but continues toward the fifth (Figs. 2-3). The three localizations from reflected angles are generally in good agreement (+/- 100 m) with the estimated track locations. The estimated depth during this track varied from 750-950 m. Swim speed during this dive approached 2.5 m s^{-1}, and the mean speed (1.7 m s^{-1}) was the fastest estimated for the ten tracks (Table II).

During track AP-1, the mean estimated angular correction for array tilt was 0.83° for the five DASBRs. If array tilt is assumed to be zero, the estimated track is shifted in space by ~0.5 km at the beginning of the track, but this track error becomes almost trivial when the animal is closer to the recorders (Fig. 3B). Without tilt correction, the track does not pass as near the localizations which are based on reflected angles (Fig. 3B). Also, in this case the initial depth is shallower (~600 m) and swimming speeds are lower without tilt correction.

The mean depth of all tracks is 967 m, but varies considerably among individual tracks (Fig. 4). The overall mean swim speed is 1.19 m s^{-1} with a range of 0.6 to 1.7 m s^{-1} among tracks (Table II). Swim directions show no obvious patterns and, in three cases, changed markedly during a dive (Fig. 5). The mean net horizontal speed (0.63 m s^{-1}) is roughly half the mean swim speed. The angular corrections for array tilt have a mean absolute value of 1.6° (Table II). Detailed plots for all ten tracks are given in supplemental material[1].

In one case (dive AI) tracks of multiple individuals were sufficiently distinct to allow each to be tracked individually[1], and dives from three individuals (or tightly associated subgroups) in this "group dive" are included separately in the sample of ten tracked dives. Dive AI had the longest period of echolocation (53 min) of all the identified dives. Track AI-1 consisted of a steep dive towards the bottom and ended at about the same time that tracks AI-2 and AI-3 began, again as descents that ended at approximately 1,000-1,100 m depth.

FIG. 2. Detection angles (relative to vertical) of beaked whale echolocation pulses measured from the TDOA from dive "AP-1" received by a vertical hydrophone array of each DASBR (filled symbols). Symbols and colors correspond to the same DASBR drifts illustrated in Fig. 3. Detection angles for reflected signals are circled and those for direct-path signals are not circled. Detection angles are averaged over 1-minute intervals and are not available for all minutes. (Color online)

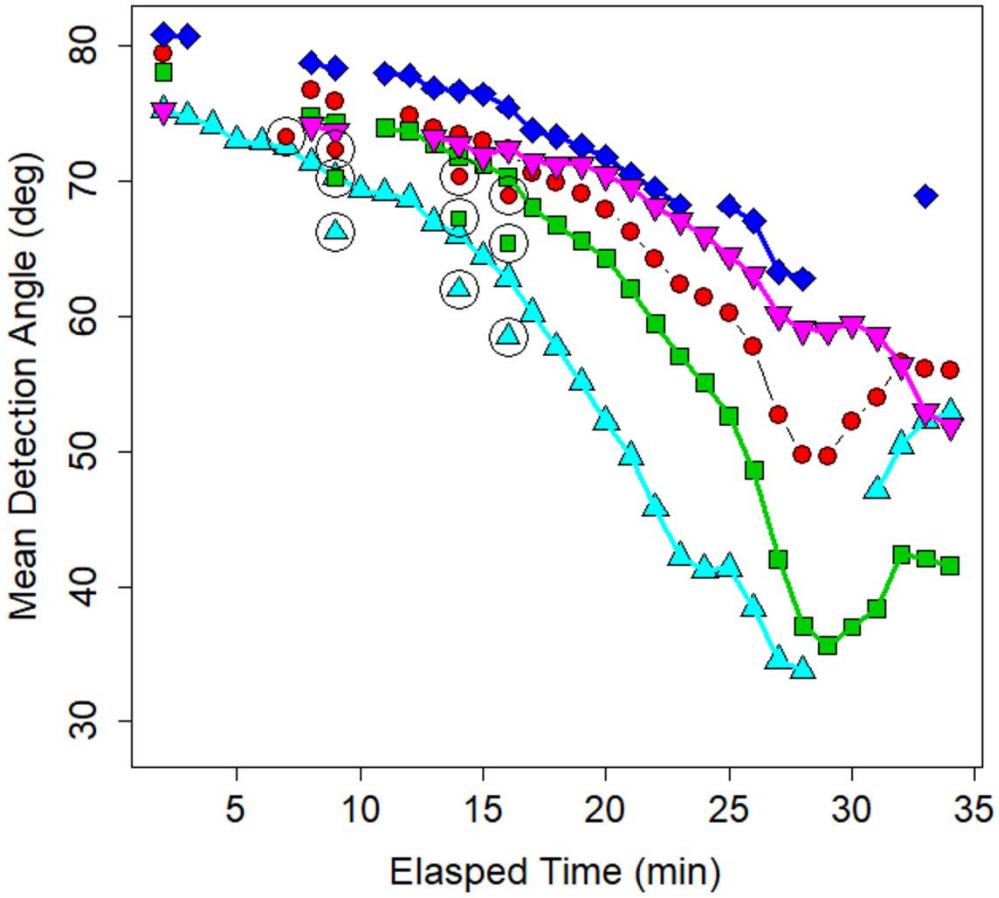

FIG. 3. DASBR drifts (colored lines) and estimated spatial tracks of a beaked whale (black line with error bars) during a 32-minute period of echolocation for dive AP-1 with (A) and without (B) correction for array tilt. Localizations based on surface reflections are illustrated as black triangles. Location error bars indicate two standard deviations from the Bayesian posterior distributions. Symbols shapes and colors at the start of each DASBR drift correspond to symbols in Fig. 2. Coordinates are for Zone 11 of the Universal Transverse Mercator system. (Color online)

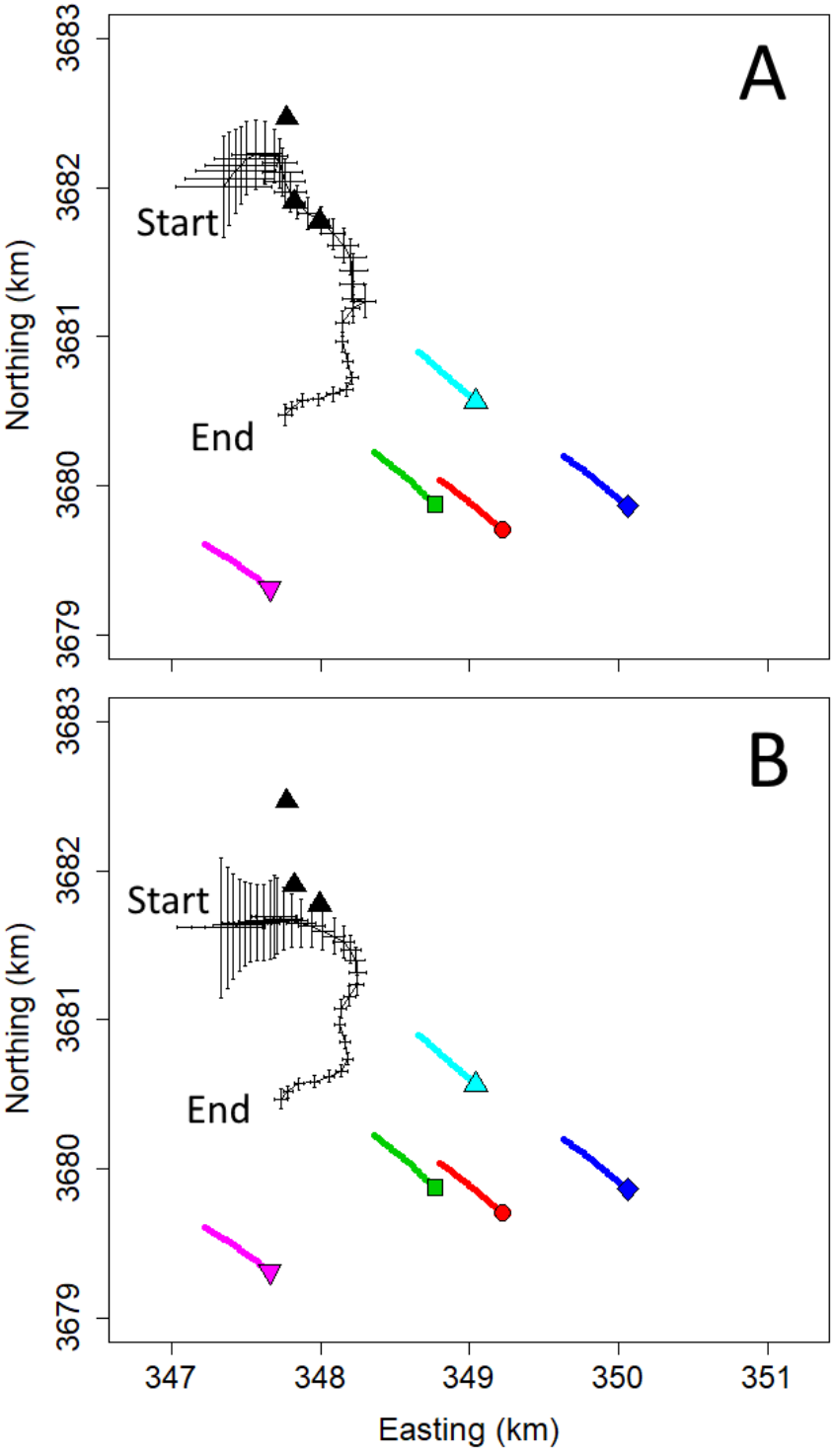

FIG. 4. Estimated depths for ten tracked beaked whale dives. Labels indicate specific dives or segments of dives (Table II). Dashed black line indicates nominal seafloor depth in the Catalina Basin. (Color online)

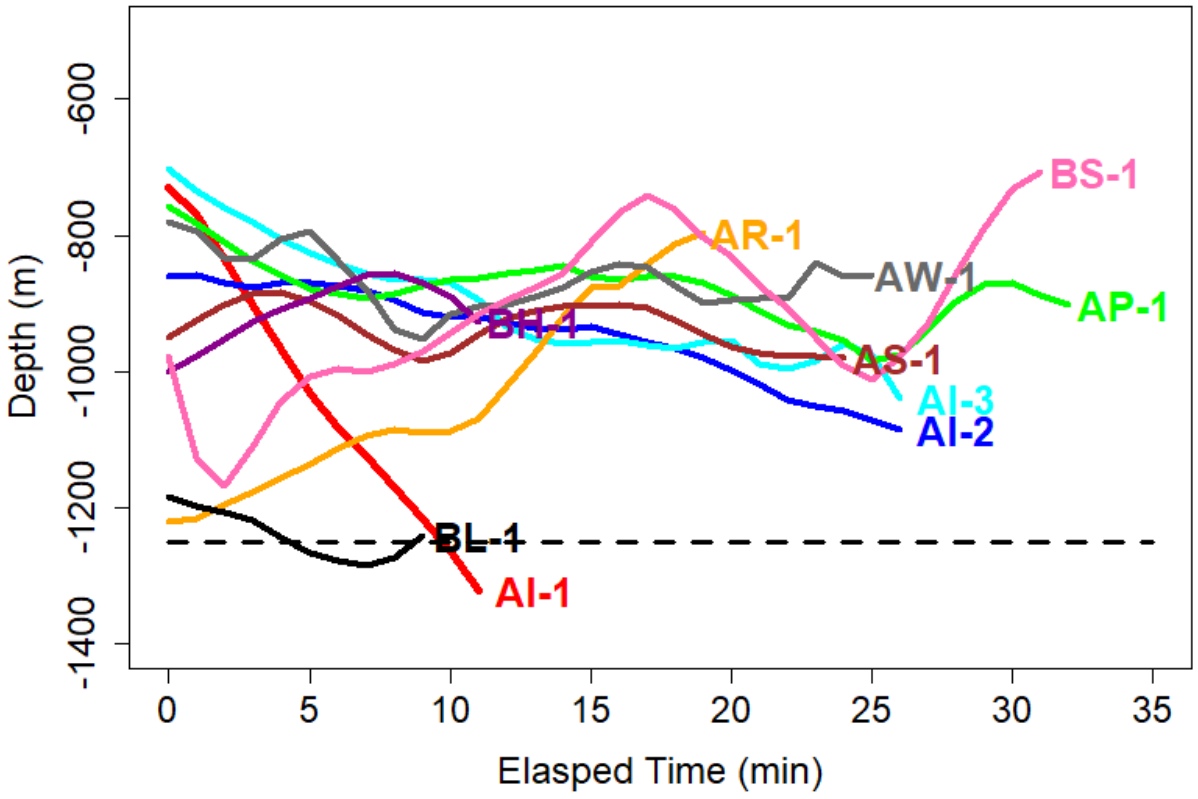

IV. DISCUSSION

A. Swimming speed

The swimming speed of Cuvier's beaked whales during foraging dives has not been directly measured from tagging studies, but rapid avoidance speeds were estimated as 2.6 and 3.1 m s^{-1} (DeRuiter et al. 2013). The descent and ascent rates for a deep dive have been measured as 1.5 and 0.7 m s^{-1} (respectively) in the Ligurian Sea (Tyack et al. 2006) and 1.4 and 0.68 m s^{-1} (respectively) off Hawaii (Baird et al. 2008); however, these are based on rates of change in depth and are not true swim speeds. From accelerometers within their tags, Tyack et al. (2006) estimate a mean decent angle of 72° and an ascent angle of 35° during deep dives. Based on these, the expected swim speeds would be 1.5-1.6 m s^{-1} on descent and ~1.2 m s^{-1} on ascent. The Gassmann et al. (2015) tracking study estimated horizontal movement speeds ranging from 1 to

3 m s^{-1}. The swim speeds estimated in our dive tracking study (mean = 1.18 m s^{-1}) are consistent with those from these previous studies of foraging behavior and are much less than speeds that have been measured during avoidance behavior. However, our estimates of swim speeds are based on net movements in 1-min time intervals and do not include the potential of course changes within that interval which would result in a slight underestimate of true foraging speeds.

FIG. 5. Track locations for ten tracked beaked whale dives relative to their start location (at the origin: 0, 0). End locations are indicated with filled circles. Labels at end locations indicate specific dives or segments of dives (Table II). (Color online)

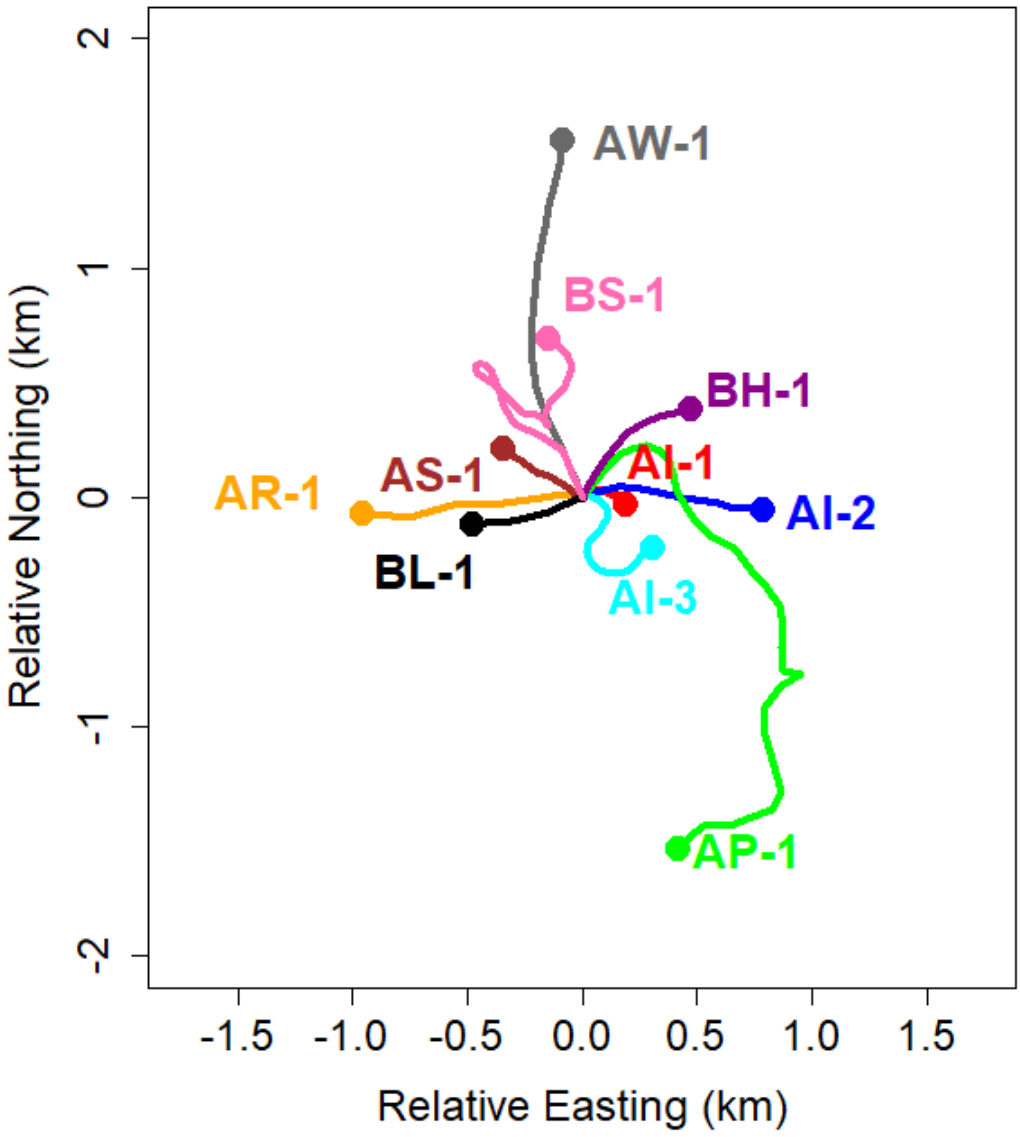

B. Foraging times

Because Cuvier's beaked whales typically produce echolocation pulses only during deep dives (Tyack et al. 2006), the duration of a period of regular pulses can be used to infer the duration of a foraging bout. In this study, it is clear that echolocation pulses cannot always be received by all hydrophones, even at relatively close range. For dive AP-1 (Fig. 2), echolocation pulses were received more consistently after 10 minutes from the start, when the animal turned towards the drifting array of hydrophones. Pulse reception became intermittent again when the animal turned away from some hydrophones at 29 minutes. Because reception of echolocation pulses varies with animal orientation and range, we cannot precisely estimate foraging times with our data.

The expected duration of the foraging portion of a deep dive can be estimated from previous tagging studies. Acoustic tagging studies have shown that regular echolocation pulses start at an average depth of 457 m on descent and ends at a depth of 856 m on ascent. Based on mean descent and ascent rates of 1.45 and 0.69 m s^{-1} (averaged from the studies cited above), echolocation pulses would begin approximately 5.3 min after the start of a deep dive and would end approximately 20.7 min before the end of the dive. If the same pattern holds elsewhere, foraging times would be approximately 26 minutes less than deep dive times. From tagging studies, the mean duration of deep dives has been estimated as 58 min (s.d. = 11 min) in the Ligurian Sea (Tyack et al. 2006), 68 min (s.d. = 9 min) off Hawaii (Baird et al. 2008), and 67 min (s.d. = 6.9) off southern California (Schorr et al. 2014). Based on these total dive times, the expected time foraging would be 32, 42, and 41 min (respectively). Warren et al. (2017) directly measured the duration of echolocation bouts in California (35.1 min, s.d. = 9.1) and the Ligurian Sea (35.2 min, s.d. = 5.7). Most of the echolocation periods on dives in this study (17 of 29) were shorter than 20 minutes and likely represent fragments of dives when the animal's range and orientation allowed detection of their echolocation signals. However, 8 of these 29 identified dives had echolocation periods longer than 30 minutes and represent a substantial portion of the expected foraging time during a deep dive.

C. Dive depths

The mean value of maximum depth per dive for the ten tracks in our study (1,104 m) is similar to the mean for Cuvier's beaked whale dives from tagging studies in the Ligurian Sea (1,070 m, Tyack et al. 2006), but is not as deep as measured for tagged whales off Hawaii (1,392 m, Baird et al. 2008) and elsewhere off southern California (1,401 m, Schorr et al. 2014). Beaked whale dives in the Catalina Basin are constrained by the depth of that basin (~1,250 m), which explains some of this difference. Although some animals in this study were foraging on or near the bottom during at least a portion of their dive (dives AI-1, AR-1 and BL-1, Fig. 4), the majority of echolocation signals were not near the seafloor. Dives AI-1 and BL-1 appear to go

below the nominal seafloor depth (Fig. 4); however, the confidence limits of theses estimated depths include the estimated seafloor depth.

In our study, the mean depth of foraging is 967 m (s.d. = 112 m, s.e. = 35.4 m). In a study area only ~100 km south and in similar water depths, the Gassmann et al. (2015) study found a mean foraging depth of 1,041m (s.d. = 140.3 m, s.e. = 42.3 m, M. Gassmann, pers. comm.). Mean foraging depth has not been reported for tagged animals, but Baird et al. (2008) reports that the mean depth when deeper than 800 m in Hawaii is 1,282 m. DeAngelis et al. (2017) found an average depth for Cuvier's beaked whales detected with towed arrays off the U.S. Atlantic coast to be 1,158 m (s.d. = 287 m). Acoustic tags in the Ligurian Sea (Tyack et al. 2006) and tracking studies using bottom-mounted hydrophones in Southern California (Gassmann et al. 2015) show that Cuvier's beaked whales start echolocation at a depth of ~500 m during their descent. None of the localizations or tracks in our study were above 600 m and only two localizations were above 700 m. Although this may indicate that echolocation starts at deeper depths in our study area, this is likely an artifact of animal orientation. The declination angle during descent has been estimated as 72° (Tyack et al. 2006), hence the main axis of their echolocation signals will be facing away from our hydrophones at 100-m depth. Near-surface hydrophones may simply be less likely to detect beaked whales during the descent phase of their deep dives.

D. Foraging strategies

Few of the individuals in this study appear to concentrate their foraging on or near the seafloor. Clearly, the seafloor at 1,250 m is within the foraging depth range of Cuvier's beaked whales; however, it appears to be used only occasionally by a few individuals. Similarly, Gassmann et al. (2015, their Fig. 6a) also showed that a Cuvier's beaked whale in southern California spent most of its time foraging ~300-400 m above the seafloor.

Our tracking data show that beaked whales can be detected on near-surface hydrophones at horizontal ranges greater than 1 km even when their net direction of travel is away from the hydrophone (Fig. 3). Previous propagation modeling by Zimmer et al. (2008) indicated that off-axis echolocation pulses are unlikely to be detected at slant ranges greater than 0.7 km. The most likely explanation for our observation is that beaked whales are not limiting their acoustic search to waters directly ahead of their net direction of travel. Our estimates of net horizontal speed of tracked whales is roughly half of their estimated swim speeds. Although some whales traveled in relatively straight lines (Fig. 5), their net horizontal speeds were still less than their mean estimated swim speeds (Table II), likely because they are turning frequently while foraging and because swim speed can have a vertical vector component. The net direction of travel underwater appeared to be random with respect to the direction of the northwesterly surface currents (Fig. 5). At 0.63 m s^{-1}, the net horizontal distance covered on a typical 40-minute foraging bout would be ~1.5 km.

E. Group foraging behavior

In most groups of Cuvier's beaked whales, individuals proved difficult to track because their detection angles plotted against time appeared so inter-braided that individuals could not be discriminated. In only one case (dive AI), detection angles appeared to be sufficiently distinct to identify three individuals or closely associated subgroups. At the one point in time when echolocation pulses from all three overlapped, they appeared to be separated by ~200-400 m. This dive period was the longest measured bout of echolocation (53 min), possibly because one subgroup (AI-1) began descending before the other two. The acoustic tracking by Gassmann et al. (2015) also showed separations of hundreds of meters between individuals within groups of Cuvier's beaked whales, with occasional convergences of individuals during a dive.

Group foraging behavior could be better studied with a different study design. If recorders were precisely synchronized, individual echolocation pulses might localized and the methods using by Gassmann et al. (2015) could be used to assign pulses and locations to specific individuals. Given that individuals can be precisely localized from surface reflections, time synchronization among recorders may be possible using echolocation pulses as timing signals.

F. Localization and tracking

This study has shown the feasibility of using echolocation pulses for localization and tracking of Cuvier's beaked whales. The combination of localization using surface-reflected signals and tracking using the more frequent direct-path signals allows some degree of correction for array tilt that would otherwise bias the estimated whale locations. However, the approach used here is a rather crude approximation. Array tilt has two components: an absolute value and an azimuth relative to the direction of the animals. With our approach, we estimate a single tilt correction as an additive error in direct-path detection angle for each DASBR. In reality, that correction should depend on the bearing to the animal relative to the azimuth of the array tilt. This under-specification of the problem likely explains why one of the localizations in Fig. 3 does not fall precisely on the estimated animal track. Ideally we would estimate both the absolute value and the azimuth of the array tilt, but we did not receive reflected signals often enough to allow estimation of both parameters. In the future, we recommend precisely measuring the absolute value of array tilt directly with 3D accelerometers fixed rigidly to each array and then estimating only the azimuth term in the tracking model.

Because surface-reflected signals were relatively rarely detected, reflected detection angles were averaged within a 2-minute time window to increase the sample size for localization and for correcting array tilt in the tracking algorithm. However, based on an average speed of 1.2 m s^{-1}, this introduces potential location errors of ~144 m. This factor, more than any other, likely determines the absolute track accuracy. For this reason, direct path angles were averaged over a shorter 1-minute time window. Although a shorter time window might improve relative accuracy of the track, the longer 2-minute window for reflected angles will still limit the absolute track

accuracy. Two approaches could improve track accuracy. If array tilt could be eliminated by using heavier weights and larger sub-surface buoys, the need for reflected angles would be eliminated, and localization could be based solely on direct-path angles. Alternatively, a single recording hydrophone near the surface (say a 10-m depth) might be able to more frequently detect surface reflected signals and allow for a shorter averaging window.

V. CONCLUSION

We have shown that acoustic localization and tracking using drifting near-surface hydrophones can be an alternative to tagging for the study of beaked whale diving behavior. Results from this study are generally consistent with results from tagging studies in southern California and other areas. We were able to measure diving behavior from ten tracks in a study that lasted just two weeks. A previous study (Gassmann et al. 2015) showed that beaked whales could also be tracked using bottom-mounted recorders. Many more echolocation pulses can be detected if the hydrophones are within the foraging plane of the whales (1,000-1,300 m depth) because more of the echolocation signals will be on-axis and detectable at greater distances. However, in most of the world's oceans, the seafloor is much farther from this optimum foraging depth than is the surface, thus beaked whale tracking with near-surface hydrophones is more generally applicable to all the world's oceans than tracking with bottom-mounted hydrophones. Our approach using near-surface hydrophones only requires measurement of declination angles and thus only requires pairs of hydrophones in a vertical array to be precisely time-synchronized. The Gassmann et al. (2015) method requires at least two 4-channel volumetric arrays that are precisely aligned and (internally) time-synchronized. Nested hydrophone arrays in both drifting and bottom-mounted configurations appear to be viable options for tracking beaked whale foraging behavior, and the optimum method is likely to vary with local conditions.

Acoustic tracking cannot be viewed as a replacement for tagging studies. Tagging provides information about the diving behavior of beaked whales when they are not vocalizing, which acoustic tracking cannot do. Also, information from pressure sensors, accelerometers and magnetometers on tags provides much more detailed information on diving behavior than our tracking data. However, despite considerable tagging effort, tagging studies have been largely limited to a few of the 22 species of beaked whale. In part, this is because the other species either do not occur in calm, near shore areas where tagging is feasible or because they do not occur in high densities. Even in calm conditions in high density areas, one or two weeks of dedicated effort may be needed to place a tag on a single individual.

We hope that acoustic tracking will be used as an alternative to tagging to study beaked whale behavior for some of the species for which tagging has not been successful. We do not know much about the diving habits of the vast majority of beaked whale species. Some only live in far offshore areas where surface conditions are often too rough for tagging. In such studies, additional effort should be considered to precisely time-synchronize the recorders and thereby obtain more information to allow tracking individuals within a group.

In addition to their use in localization and tracking, drifting recording systems have many other uses in studies of cetacean behavior, distribution and abundance. In a larger-scale study, DASBRs have been used to identify a new beaked whale echolocation pulse type (Griffiths et al., in press) and to map the distribution of this and other known beaked whale pulse types in the California Current (Keating et al. 2018). Drifting buoy systems can be used to study distribution and relative abundance of cetaceans in ocean basins where seafloor hydrophone recorders are impractical or ineffective due to the depth of the seafloor. Ultimately, we hope to use drifting hydrophone recorders to estimate the density and abundance of beaked whales, sperm whales, and other cetacean species.

ACKNOWLEDGMENTS

Funding for this research was provided by the U.S. Office of Naval Research (Project #N00014-15-1-2142 and MIPR #N0001416IP00059) and NOAA's Southwest Fisheries Science Center. Vessel time on the Horizon was funded by NOAA's Cooperative Research Program. Funding for DASBR development and some equipment was provided by the U.S. Navy's N45 and Living Marine Resource programs and by NOAA's Acoustics Program. We thank Mike Weise, Frank Stone, Jason Gedamke, Lisa Ballance, and Anu Kumar for their support. Field assistance was provided by Selene Fregosi, Dave Mellinger, Jennifer Keating, and Eiren Jacobson. Vessel operators were Trevor Oudin, Juan Carlos Aguilar, and Spencer Salmon. The Bayesian tracking algorithm was inspired by OpenBUGS code published by Laplanche et al. (2015). Jeff Moore helping in implementing the R2OpenBUGS package. This manuscript was improved by helpful reviews from Jeff Moore, Selene Fregosi, and three anonymous reviewers.

[1] See supplementary material at [URL will be inserted by AIP] for a more detailed table with times and durations of all acoustically detected foraging dives, BUGS code for the tracking algorithm, and additional color plots illustrating the detection angles, x-y-z locations, and speeds for all ten tracked dives.

Baggenstoss, P. M. (**2011**). "An algorithm for the localization of multiple interfering sperm whales using multi-sensor time difference of arrival," J. Acoust. Soc. Am. **130**:102-112.

Baird, R. W., Webster, D. L., Schorr, G. S., McSweeney, D. J., and Barlow, J. (**2008**). "Diel variation in beaked whale diving behaviour," Marine Mammal Sci. **24**, 630-642.

Barlow, J. and Griffiths, E. T. (**2017**). "Precision and bias in estimating detection distances for beaked whale echolocation clicks using a two-element vertical hydrophone array," J. Acoust. Soc. Am. **141**:4388-4397.

Baumann-Pickering, S, McDonald MA, Simonis AE, Berga AS, Merkens KPB, Oleson EM, Roch MA, Wiggins SM, Rankin S, Yack TM, Hildebrand JA. (**2013**). "Species-specific beaked whale echolocation signals," J. Acoust. Soc. Am. **134**:2293-2301.

Baumann-Pickering, S., Roch, M.A., Brownell Jr, R.L., Simonis, A.E., McDonald, M.A., Solsona-Berga, A., Oleson, E.M., Wiggins, S.M. and Hildebrand, J.A. (**2014**). "Spatio-temporal patterns of beaked whale echolocation signals in the North Pacific," PloS one, **9(1)**, p.e86072.

Carnes, M.R. (**2009**). "Description and Evaluation of GDEM-V 3.0," Naval Research Laboratory Memorandum Report NRL/MR/7330-09-9165. 21pp.

Cato, D. H. (**1998**). "Simple methods of estimating source levels and locations of marine animal sounds," J. Acoust. Soc. Am. **104**:1667-1678.

DeAngelis, A. I., Valtierra, R., Van Parijs, S. M., and Cholewiak, D. (**2017**). Using multipath reflections to obtain dive depths of beaked whales from a towed hydrophone array. J. Acoust. Soc. Am. **142**:1078-1087.

DeRuiter, S. L., Southhall, B. L., Calambokidis, J., Zimmer, W. M. X., Sadykova, D., Falcone, E. A., Friedlaender, A. S., Joseph, J. E., Moretti, D., Schorr, G. S., Thomas, L., and Tyack, P. L. (**2013**). "First direct measurements of behavioral responses by Cuvier's beaked whales to mid-frequency active sonar," Biol. Lett. **9**:20130223.

Frantzis, A., Goold, J. C., Skarsoulis, E. K., Taroudakis, M. I., and Kandia, V. (**2002**). "Clicks from Cuvier's beaked whales, *Ziphius cavirostris* (L)," J. Acoust. Soc. Am. **112:**34-37.

Gassmann, M., Henderson, E., Wiggins, S. M., Roch, M. A., and Hildebrand, J. A. (**2013**). "Offshore killer whale tracking using multiple hydrophone arrays," J. Acoust. Soc. Am. **134**:3513-3521.

Gassmann. M., Wiggins, S. M., and Hildebrand, J. A. (**2015**). "Three-dimensional tracking of Cuvier's beaked whales' echolocation sounds using nested hydrophone arrays," J. Acoust. Soc. Am. **138**:2483-2494.

Gillespie, D., Mellinger, D. K., Gordon, J., Mclaren, D., Redmond, P. , McHugh, R., Tinder, P., Deng, X.-Y., and Thode, A. (**2008**). "PAMGUARD: Semiautomated, open source software for real-time acoustic detection and localisation of cetaceans," J. Acoust. Soc. Am. **30**:54-62.

Griffiths, E. T. and Barlow J. (**2015**). "Equipment performance report for the drifting acoustic spar buoy recorder (DASBR)," NOAA Technical Memorandum NOAA-TM-NMFS-SWFSC-543. 36pp.

Griffiths, E. T. and Barlow J. (**2016**). "Cetacean acoustic detections from free-floating vertical hydrophone arrays in the southern California Current," J. Acoust. Soc. Am. Electronic Letters.

Griffiths, E. T., Keating, J. L., Barlow, J., and Moore, J. E. (in press). "Description of a new beaked whale echolocation pulse type in the California Current," Marine Mammal Science.

Johnson, M, Madsen, P. T., Zimmer, W. M. X., Aguilar de Soto, N., and Tyack, P. L. (**2004**). "Beaked whales echolocate on prey," Proceedings Royal Society, London, B (Supplement 6): S383 - S386.

Johnson, M., Hickmott, L. S., Aguilar Soto, N., and Madsen, P. T. (**2008**). "Echolocation behavior adapted to prey in foraging Blainville's beaked whale (*Mesoplodon densirostris*)," Proc. R. Soc., B **275**:133-139.

Keating, J. L. and Barlow, J. (**2013**). "Click detectors and classifiers used during the 2012 southern California behavioral response study," NOAA Technical Memorandum NOAA-TM-NMFS-SWFSC-517. 14pp.

Keating J.L., Barlow, J., Griffiths, E.T., and Moore, J.E. (**2018**). "Passive Acoustics Survey of Cetacean Abundance Level (PASCAL-2016) Final Report," Honolulu (HI): US Department of the Interior, Bureau of Ocean Energy Management. OCS Study BOEM 2018-025. 33p.

Laplanche, C., Marques, T. A., and Thomas, L. (**2015**). "Tracking marine mammals in 3D using electronic tags," Methods in Ecol. and Evol. **6**:987-996.

Lunn, D., Jackson, C., Best, N., Thomas, A., & Spiegelhalter, D. (**2012**). *The BUGS book: A practical introduction to Bayesian analysis*. CRC Press. 399pp.

Lunn, D., Spiegelhalter, D., Thomas, A. and Best, N. (**2009**). "The BUGS project: Evolution, critique and future directions (with discussion)," Statistics in Medicine **28**: 3049--3082.

MacDonald, I. L., & Zucchini, W. (**1997**). *Hidden Markov and other models for discrete-valued time series.* Monographs on Statistics and Applied Probability 70. Chapman and Hall, London. 236pp

McGehee, D. E. (**2000**). "Simple methods for locating, counting, and tracking sperm whales underwater in three dimensions," J. Acoust. Soc. Am. **108**:2540.

Miller, B., and Dawson, S. (**2009**). "A large-aperture low-cost hydrophone array for tracking whales from small boats," J. Acoust. Soc. Am. **126**:2248-2256.

Møhl, B., Wahlberg, M, Madsen, P. T., Miller, L. A., and Surlykke, A. (**2000**). "Sperm whale clicks: directionality and source level revisited," J. Acoust. Soc. Am. **107**:638-648.

Møhl, B., Wahlberg, M., and Heerfordt, A. (**2001**). "A large-aperture array of nonlinked receivers for acoustic positioning of biological sound sources," J. Acoust. Soc. Am. **109**:434-437.

Nosal, E.-M., and Frazer, L. N. (**2007**). "Sperm whale three-dimensional track, swim orientation, beam pattern, and click levels observed on bottom-mounted hydrophones," J. Acoust. Soc. Am. **112**:1969-1978.

R Core Team. (2013). " R: A language and environment for statistical computing." R Foundation of Statistical Computing, Vienna, Austria. URL http://www.R-project.org/.

Schorr, G. S., Falcone, E. A., Moretti, D. J., and Andrews, R. D. (**2014**). "First long-term behavioral records from Cuvier's beaked whales (*Ziphius cavirostris*) reveal record-breaking dives," PLOS One **9**:e92633.

Sueur J., Aubin T., Simonis C. (**2008**). "Seewave: a free modular tool for sound analysis and synthesis," Bioacoustics **18**: 213-226

Thode, A. (**2004**) "Tracking sperm whale (*Physeter macrocephalus*) dive profiles using a towed passive acoustic array," J. Acoust. Soc. Am. **116**:245-253.

Tyack, P. L., Johnson, M., Soto, N. A., Sturlese, A., and Madsen, P. T. (**2006**). "Extreme diving behaviour of beaked whales," J. Exp. Biol. **209**, 4238–4253.

Wahlberg, M., Møhl, B., and Madsen, P. T. (**2001**). "Estimating source position accuracy of a large-aperture hydrophone array for bioacoustics," J. Acoust. Soc. Am. **109:**397-406.

Ward, J., Morrissey, R., Moretti, D., DiMarzio, N., Jarvis, S., Johnson, M., Tyack, P. and White, C. (**2008**). "Passive acoustic detection and localization of *Mesoplodon densirostris* (Blainville's beaked whale) vocalization using distributed bottom-mounted hydrophones in conjunction with a digital tag (DTAG) recording," Canadian Acoustics **36**:60-66.

Warren, V. E., Marques, T. A., Harris, D., Thomas, L., Tyack, P. L., Aguilar de Soto, N, Hickmott, L. S., and Johnson, M. P. (**2017**). "Spatio-temporal variation in click production rates of beaked whales: Implications for passive acoustic density estimation," J. Acoust. Soc. Am. **141**:1962-1974.

Yack, T. M., Barlow, J. Calambokidis, J, Southhall, B., and Coates, S. (**2013**). "Passive acoustic monitoring using a towed hydrophone array results in identification of a previously unknown beaked whale habitat," J. Acoust. Soc. Am. **134**: 2589–2595.

Yack, T. M., Barlow, J., Roch, M. A., Klinck, H., Martin, S., Mellinger, D. K., and Gillespie, D. (**2010**). "Comparison of beaked whale detection algorithms," Appl.Acoust. **71**:1043-1049.

Zimmer, W. M., Harwood, J., Tyack, P. L., Johnson, M. P., and Madsen, P. T. (**2008**). "Passive acoustic detection of deep diving beaked whales," J. Acoust. Soc. Am. **124**, 2823–2832.

Zimmer, W.M. and Pavan, G. (**2008**). "Context driven detection/classification of Cuvier's beaked whale (*Ziphius cavirostris*)," In *New Trends for Environmental Monitoring Using Passive Systems, 2008* (pp. 1-6).

TABLE I. Localizations of Cuvier's beaked whales from declination angles estimated from surface-reflected echolocation pulses. Latitude, longitude and depth are estimated by finding the best convergence of bearing angles from 3 or more drifting instruments. The minimum and maximum distances from the estimated location to the instruments are also given. Localizations from only three instruments are used only if unambiguously determined (only one solution at plausible depths >500m & less than the bottom depth).

Dive Label	# DASBRs with Surface Reflections	UTC Date & Time	Latitude	Longitude	Depth (m)	Min. Distance (km)	Max. Distance (km)
AI-1	4	7/22/2016 3:57	33.252	-118.618	1191	1.40	2.49
AI-2	4	7/22/2016 4:24	33.253	-118.610	952	1.42	2.54
AJ-5	3	7/22/2016 6:28	33.247	-118.640	810	0.43	1.42
AP-1	3	7/24/2016 6:16	33.270	-118.634	953	2.16	2.99
AP-1	3	7/24/2016 6:21	33.265	-118.634	854	1.60	2.39
AP-1	3	7/24/2016 6:23	33.264	-118.632	836	1.36	2.17
AR-1	3	7/24/2016 20:30	33.156	-118.556	1193	2.07	3.10
AS-1	4	7/24/2016 23:43	33.176	-118.568	734	1.88	3.45
AW-1	3	7/25/2016 7:54	33.204	-118.633	959	2.52	3.44
AW-1	3	7/25/2016 7:55	33.204	-118.634	925	2.50	3.41
AW-1	3	7/25/2016 8:10	33.216	-118.632	840	1.70	3.43
AY-1	4	7/25/2016 10:57	33.262	-118.674	1085	1.36	2.85
AY-1	4	7/25/2016 11:08	33.259	-118.674	1067	1.34	2.48
AY-1	5	7/25/2016 11:14	33.259	-118.666	1247	1.62	2.80
AY-1	4	7/25/2016 11:20	33.257	-118.678	693	1.12	2.07
BH-1	4	7/26/2016 9:19	33.226	-118.670	976	2.17	3.48
BH-2	4	7/26/2016 9:39	33.225	-118.663	954	1.47	2.62
BL-1	4	7/27/2016 8:11	33.255	-118.604	1169	1.22	2.53
BL-1	4	7/27/2016 8:19	33.254	-118.608	1244	0.87	2.19
BM-2	3	7/27/2016 11:11	33.275	-118.638	671	0.74	1.64
BM-3	4	7/27/2016 11:15	33.263	-118.630	1136	1.03	2.16
BS-1	4	7/29/2016 12:44	33.224	-118.653	1046	1.00	2.46
BS-1	4	7/29/2016 13:07	33.226	-118.650	933	1.26	2.56
		Average			977	1.49	2.64
		Standard Deviation			171	0.54	0.57
		Standard Error			36	0.11	0.12
		Maximum			1247	2.52	3.48
		Minimum			671	0.43	1.42

TABLE II. Summary statistics for each of ten dive tracks. The net distance traveled is based only on the beginning and ending position of a track, and the net horizontal speed is estimated as the net distance divided by the duration of the track. The RMS angle error is the root-mean-squared difference between the observed direct path angles and those predicted by the fitted track and includes both systematic error due to array tilt and measurement error.

Dive	Duration (min)	Mean Speed ($m\ s^{-1}$)	Mean Depth (m)	Maximum Depth (m)	Net Distance Traveled (km)	Net Horizontal Speed ($m\ s^{-1}$)	Mean Absolute Tilt Correction (deg)	RMS Angle Error (deg)
AI-1	11	1.18	1035	1323	0.19	0.29	2.22	2.52
AI-2	26	0.64	945	1085	0.79	0.51	1.80	1.92
AI-3	26	0.87	902	1040	0.38	0.24	2.39	3.30
AP-1	32	1.69	879	984	1.59	0.83	0.83	1.02
AR-1	19	1.26	1038	1222	0.96	0.84	1.09	1.37
AS-1	24	0.70	935	984	0.40	0.28	1.11	1.17
AW-1	25	1.57	865	952	1.56	1.04	1.04	1.50
BH-1	11	1.28	911	1001	0.61	0.93	2.46	3.13
BL-1	9	1.14	1240	1286	0.49	0.92	1.14	1.73
BS-1	31	1.61	916	1168	0.71	0.38	2.22	2.39
mean	21.4	1.19	967	1104	0.77	0.63	1.63	2.01
s.d.	8.4	0.37	112	136	0.48	0.31	0.65	0.80

Figure Captions

FIG. 1. Drifts of buoy recorders in the Catalina Basin (white lines). Eight buoys were typically deployed in a 2 x 4 rectangular configuration separated by ~ 900 m (as exemplified by black and white circle symbols) and drifted northeast. Black and white square symbols indicate localized Cuvier's beaked whales (Table I). Drifts were designed to pass over two seafloor recorders (triangles) as part of a different study.

FIG. 2. Detection angles (relative to vertical) measured from the TDOA from dive "AP-1" received by a vertical hydrophone array of each DASBR (filled symbols). Symbols and colors correspond to the same DASBR drifts illustrated in Fig. 3. Detection angles for reflected signals are circled and those for direct-path signals are not circled. Detection angles are averaged over 1-minute intervals and are not available for all minutes. (Color online)

FIG. 3. DASBR drifts (colored lines) and estimated spatial tracks of beaked whales (black line with error bars) during a 32-minute period of echolocation for dive AP-1 with (A) and without (B) correction for array tilt. Localizations based on surface reflections are illustrated as black triangles. Location error bars indicate two standard deviations from the Bayesian posterior distributions. Symbols and colors at the start of each DASBR drift correspond to symbols in Fig. 2. Coordinates are for Zone 11 of the Universal Transverse Mercator system. (Color online)

FIG. 4. Estimated depths for ten tracked beaked whale dives. Labels indicate specific dives or segments of dives (Table II). (Color online)

FIG. 5. Track locations for ten tracked beaked whale dives relative to their start location (at the origin: 0, 0). End locations are indicated with filled circles. Labels at end locations indicate specific dives or segments of dives (Table II). (Color online)

Supplementary Material 1

Fitting state-space models by MCMC using OpenBugs

State-space models describe the state of a complex dynamic system, for example the location in space of a moving object. Often the state cannot be measured directly without error (described as a hidden state), but aspects related to that state can be measured. In our example, the state is the location of an echo-locating beaked whale as it dives and forages. The data that provide information about that state are the declination angles to the whales (measured from the time-difference-of-arrival (TDOA) of an echolocation pulse on two hydrophones in a drifting vertical array or from the TDOA of a pulse and its surface reflection arriving on a single hydrophone) and the locations where these angles were measured.

Historically, state-space models have been fit to data using three methods: Kalman filters, Sequential Monte Carlo (SMC, often referred to as a particle filter), and Markov Chain Monte Carlo (MCMC), although hybrid methods are now being developed (Andrieu et al. 2010). Here I provide a brief, simplified description of these three approaches. Kalman filters (Kalman 1996) were developed first and require the least processing power. In a Kalman filter, a complex non-linear motion problem is linearized using a Taylor-series approximation, and parameters are fit using linear least-squares methods. Measurement errors in a Kalman filter model are assumed to have a Gaussian distribution. In a typical real-time application, such as rocket tracking, previous data are used to estimate a current state. SMC (Del Moral et al. 2008) is similar in that it is applied sequentially to estimate a state based on previous states but is more general than the Kalman filter and allows for non-Gaussian error distributions. Unlike the Kalman filter, SMC is considered to be a Bayesian method in that inferences are based on posterior densities. In SMC, posterior densities are approximated sequentially using previous data (Andrieu et al. 2010). Posterior densities are built from distributions of many samples (particles). MCMC is similar in being Bayesian, in inferring states based on posterior distributions that are built of many samples, and in accommodating non-Gaussian error distributions. However, MCMC model fitting is not sequential and subsequent data can provide information on a previous state. Clearly SMC and MCMC are closely related, but the MCMC approach can be considered a simultaneous fit to all data rather than a sequential fit to previous data. SMC methods are much faster than MCMC methods, but do not use as much information. Because processing speed was not a primary consideration for our analyses, we chose to use the MCMC method.

OpenBUGS is an open-source, free software package for fitting MCMC models[d]. It evolved from a similar Microsoft Windows based package called WinBUGS (Lunn et al. 2009). Both use Gibbs samplers for analyzing the specified model. The input to this software is a statistical model

[d] http://www.openbugs.net/

specification language called BUGS, which is similar to that used previously in WinBUGS. Our BUGS model specification is given in Supplemental 2.

References

Andrieu, C., Doucet, A., & Holenstein, R. (**2010**). “Particle Markov chain Monte Carlo methods”. Journal of the Royal Statistical Society: Series B (Statistical Methodology), 72(3), 269-342.

Del Moral, P., Doucet, A., and Jasra, A. (**2008**). “On adapative resampling procedures for sequential Monte Carlo methods”. Bernoulli. 18 (1): 252–278.

Gelfand, A.E., Smith, A.F.M. (**1990**). "Sampling-based approaches to calculating marginal densities". Journal of the American Statistical Association. 85: 398–409

Kalman, R. E. (**1960**). "A new approach to linear filtering and prediction problems". Journal of Basic Engineering. 82: 35.

Lunn, D., Spiegelhalter, D., Thomas, A. and Best, N. (**2009**) “The BUGS project: Evolution, critique and future directions (with discussion)”, Statistics in Medicine 28: 3049--3082.

Supplementary Material 2

BUGS model specification for whale tracking using detection angles.

```
#NOTE: this version works OK, used in publication
# sd in angles from Barlow & Griffiths
model track {
  pi<- 3.1415926535
  twopi<- pi*2

# initial location of whale (km) based on normal prior (NOTE: depth is positive)
  sdXY<- 1
  sdZ<- 0.3
  tauXY<- pow(sdXY,-2)
  tauZ<-  pow(sdZ,-2)
  x[1]~ dnorm(startEasting,tauXY)
  y[1]~ dnorm(startNorthing,tauXY)
  z[1]~ dnorm(startDepth,tauZ)

# intitial whale speed (m / sec), speed is limited to biologically feasible
  Speed[1]~ dunif(0.25,3.5)

# initial pitch is random half-circle; zero is straight down; time step is 60 sec
  Pitch[1]~ dunif(0,pi)

# initial direction is random cicular in xy plane
  Heading[1]~ dunif(0,twopi)

# initial velocity vectors (km per 60 sec time step) from speed, pitch and heading
  vz[1]<-    Speed[1] * (60/1000) * cos(Pitch[1])
  xySpeed[1]<- Speed[1] * sin(Pitch[1])
  vx[1]<- xySpeed[1] * (60/1000) * cos(Heading[1])
  vy[1]<- xySpeed[1] * (60/1000) * sin(Heading[1])

# whale location (km) based on previous time and velocity (per time step)
  for (iTime in 1:(nTime-1)) {
    x[iTime+1]<- x[iTime] + vx[iTime]
    y[iTime+1]<- y[iTime] + vy[iTime]
    z[iTime+1]<- z[iTime] + vz[iTime]
  }

# movement xyz-velocity model standard deviations
  sdSpeed~   dunif(0.1,1.0)
  sdHeading~ dunif(0.05,1.0)
  sdPitch~   dunif(0,1.5)
  tauSpeed<-   pow(sdSpeed,-2)
  tauHeading<- pow(sdHeading,-2)
  tauPitch<-   pow(sdPitch,-2)

  for (iTime in 1:(nTime-1)) {

# pitch & heading & speed based on previous values plus deltas
    Pitch[iTime+1]~    dnorm(Pitch[iTime],tauPitch)T(0,pi)
    Heading[iTime+1]~  dnorm(Heading[iTime],tauHeading)
```

```
    Speed[iTime+1]~    dnorm(Speed[iTime],tauSpeed)T(0.25,3.5)

# horizontal speed based on total speed and pitch
    xySpeed[iTime+1]<- Speed[iTime+1] * sin(Pitch[iTime+1])

# velocities (in km per 60 sec time step) from speeds, heading, and pitch angle
    vz[iTime+1]<-   Speed[iTime+1] * (60/1000) * cos(Pitch[iTime+1])
    vx[iTime+1]<- xySpeed[iTime+1] * (60/1000) * cos(Heading[iTime+1])
    vy[iTime+1]<- xySpeed[iTime+1] * (60/1000) * sin(Heading[iTime+1])

  }

# apparent array tilt for each DASBR instrument (select between two options)
#Option 1: if no surface reflections, eliminate tilt estimation by making it trivial
  sdTilt[1]<- 0.001 * pi / 180
#Option 2: if surface reflections are available, estimate array tilt
  sdTilt[2]<- 5 * pi / 180
#Select option: test if SurfRefl variable is 1 or -1 (if statements are not allowed)
  EstTilt<- 1 + step(SurfRefl)
  tauTilt<- pow(sdTilt[EstTilt],-2)
#tilt correction for each DASBR instrument if surf reflections are available
  for (iDASBR in 1:nDASBR) {
    Tilt[iDASBR]~ dnorm(0,tauTilt)  #normal prior with zero mean
  }

# goodness of fit for predicted to observed declination angles
  tauAngle<- pow(0.8*pi/180,-2)     #informative based on Barlow&Griffiths study
sd=0.8 deg
  tauReflAngle<- pow(0.1*pi/180,-2)  #informative based on Barlow&Griffiths study
sd=0.1 deg

  for (iDASBR in 1:nDASBR) {
    for (iTime in 1:nTime) {
  # calculate horizontal range to each DASBR instrument
      range[iTime,iDASBR]<- sqrt(pow((x[iTime]-x_DASBR[iTime,iDASBR]),2) +
pow((y[iTime]-y_DASBR[iTime,iDASBR]),2))
  # direct path goodness of fit
      predAngl[iTime,iDASBR]<- arctan(range[iTime,iDASBR]/(z[iTime]-
z_DASBR[iTime,iDASBR])) + Tilt[iDASBR]
      obsAngl[iTime,iDASBR]~   dnorm(predAngl[iTime,iDASBR],tauAngle)
  # reflected angles goodness of fit
      predReflAngl[iTime,iDASBR]<- arctan(range[iTime,iDASBR]/(z[iTime]))
      ReflAngl[iTime,iDASBR]~ dnorm(predReflAngl[iTime,iDASBR],tauReflAngle)
    }
  }
}
```

Supplementary Material 3. Table of all Ziphius dives detected acoustically

Table S1. Detection of distinct echolocation periods (dives) for Cuvier's beaked whales detected on drifting acoustic recorders. Echolocation duration is the time from the first to the last pulse in what is interpreted to be a single foraging dive (often with multiple animals). Time since the previous dive ended is not calculated (n/c) for the first dive on each deployment. The number of DASBR instruments that detected each dive is also given. Highlighted dives are used for localization (Table I in the published version).

Dive Label	Deployment	Start Time (UTC)	End Time (UTC)	Echolocation Duration (min)	Time Since Previous Dive Ended (min)	# DASBRs
AA	1	7/19/2016 17:52	7/19/2016 17:54	1.77	n/c	3
AB	1	7/19/2016 19:18	7/19/2016 20:08	49.57	84.25	4
AC	1	7/19/2016 21:16	7/19/2016 21:22	5.43	68.83	3
AD	1	7/19/2016 23:41	7/19/2016 23:59	18.22	139.15	2
AE	1	7/20/2016 5:24	7/20/2016 5:35	11.27	324.72	2
AG	1	7/20/2016 12:41	7/20/2016 12:54	12.13	426.37	2
AH	3	7/21/2016 20:20	7/21/2016 20:20	0.10	n/c	2
AI	3	7/22/2016 3:48	7/22/2016 4:41	53.27	448.18	5
AJ	3	7/22/2016 6:19	7/22/2016 6:47	27.80	97.73	4
AN	4	7/23/2016 7:51	7/23/2016 7:53	1.73	n/c	2
AO	4	7/23/2016 14:34	7/23/2016 14:49	14.95	400.95	1
AP	5	7/24/2016 6:09	7/24/2016 6:45	35.45	n/c	5
AR	6	7/24/2016 20:28	7/24/2016 20:56	27.67	n/c	5
AS	6	7/24/2016 23:05	7/24/2016 23:45	39.22	129.78	4
AT	6	7/25/2016 3:49	7/25/2016 4:11	22.47	244.30	2
AU	6	7/25/2016 5:14	7/25/2016 5:18	4.08	62.45	2
AV	6	7/25/2016 6:09	7/25/2016 6:27	18.20	50.73	3
AW	6	7/25/2016 7:50	7/25/2016 8:11	20.68	82.95	4
AX	6	7/25/2016 9:10	7/25/2016 9:18	7.48	59.77	3
AY	6	7/25/2016 10:53	7/25/2016 11:30	36.50	95.48	5
BH	7	7/26/2016 9:18	7/26/2016 10:00	41.98	n/c	4
BJ	8	7/27/2016 4:35	7/27/2016 4:47	12.62	n/c	2
BL	8	7/27/2016 8:10	7/27/2016 8:20	10.17	202.47	4
BM	8	7/27/2016 11:06	7/27/2016 11:17	11.53	165.53	4
BN	9	7/28/2016 2:30	7/28/2016 2:32	2.28	n/c	3
BO	9	7/28/2016 4:32	7/28/2016 4:41	8.85	119.67	2
BP	9	7/28/2016 7:08	7/28/2016 7:16	8.17	147.67	2
BQ	9	7/28/2016 10:35	7/28/2016 11:10	34.80	198.62	2
BS	10	7/29/2016 12:41	7/29/2016 13:14	32.37	n/c	5

Supplementary Material 4. Additional figures.

FIG. S1. Estimated speeds through the water for ten tracked beaked whale dives. Labels and colors indicate specific dives or segments of dives (Table II).

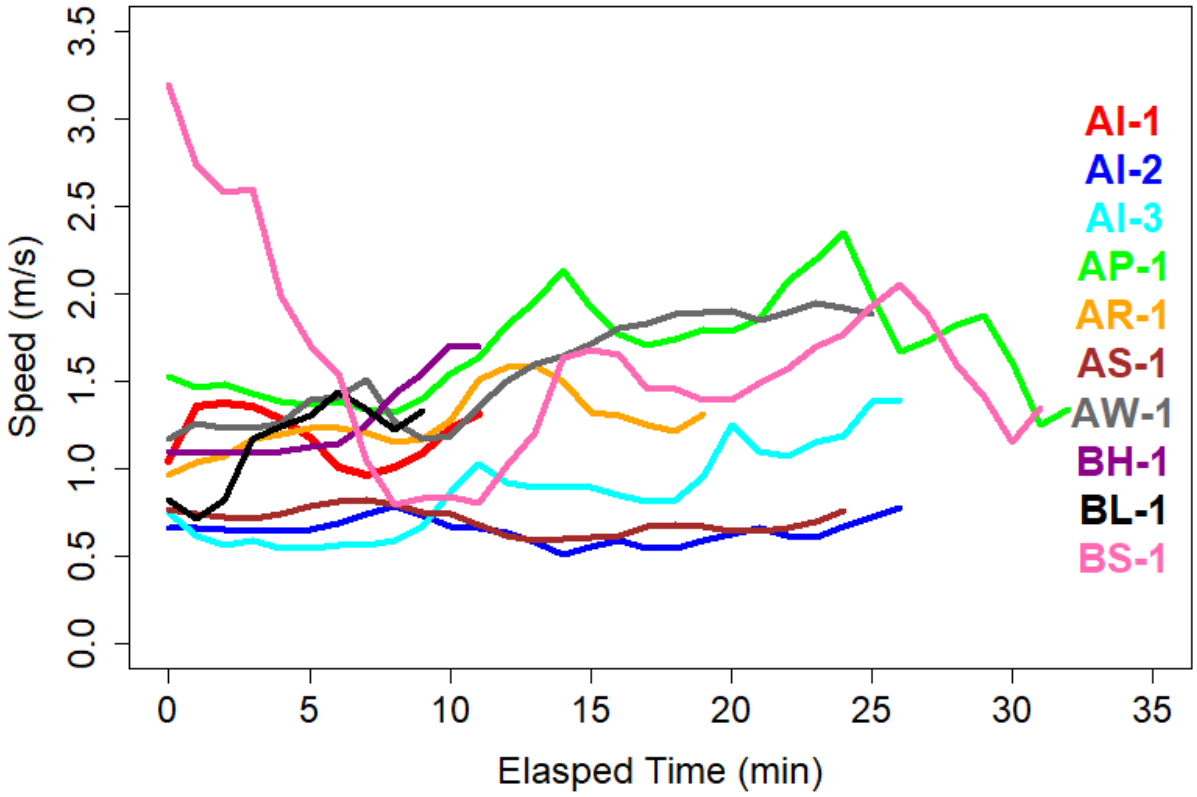

Supplementary Material 4. Additional figures.

FIG. S2. Detection angle data, estimated location track, estimated depth and estimated speed through the water for track AI-1. See figure captions for Fig. 2, 3, 5, and S1 for detailed explanation of each panel. Error bars are two standard deviations in the posterior distribution.

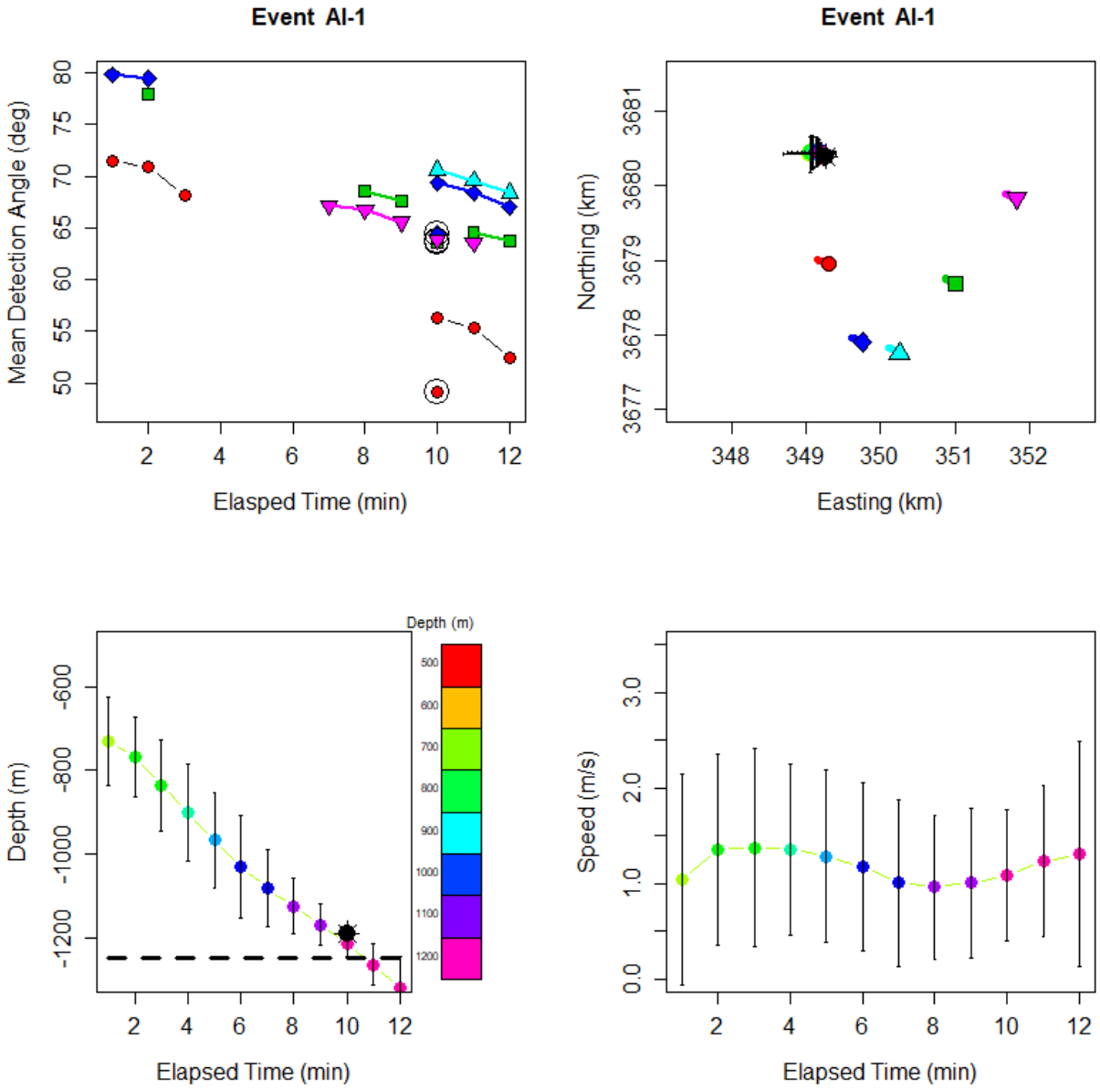

Supplementary Material 4. Additional figures.

FIG. S3. Detection angle data, estimated location track, estimated depth and estimated speed through the water for track AI-2. See figure captions for Fig. 2, 3, 5, and S1 for detailed explanation of each panel. Error bars are two standard deviations in the posterior distribution.

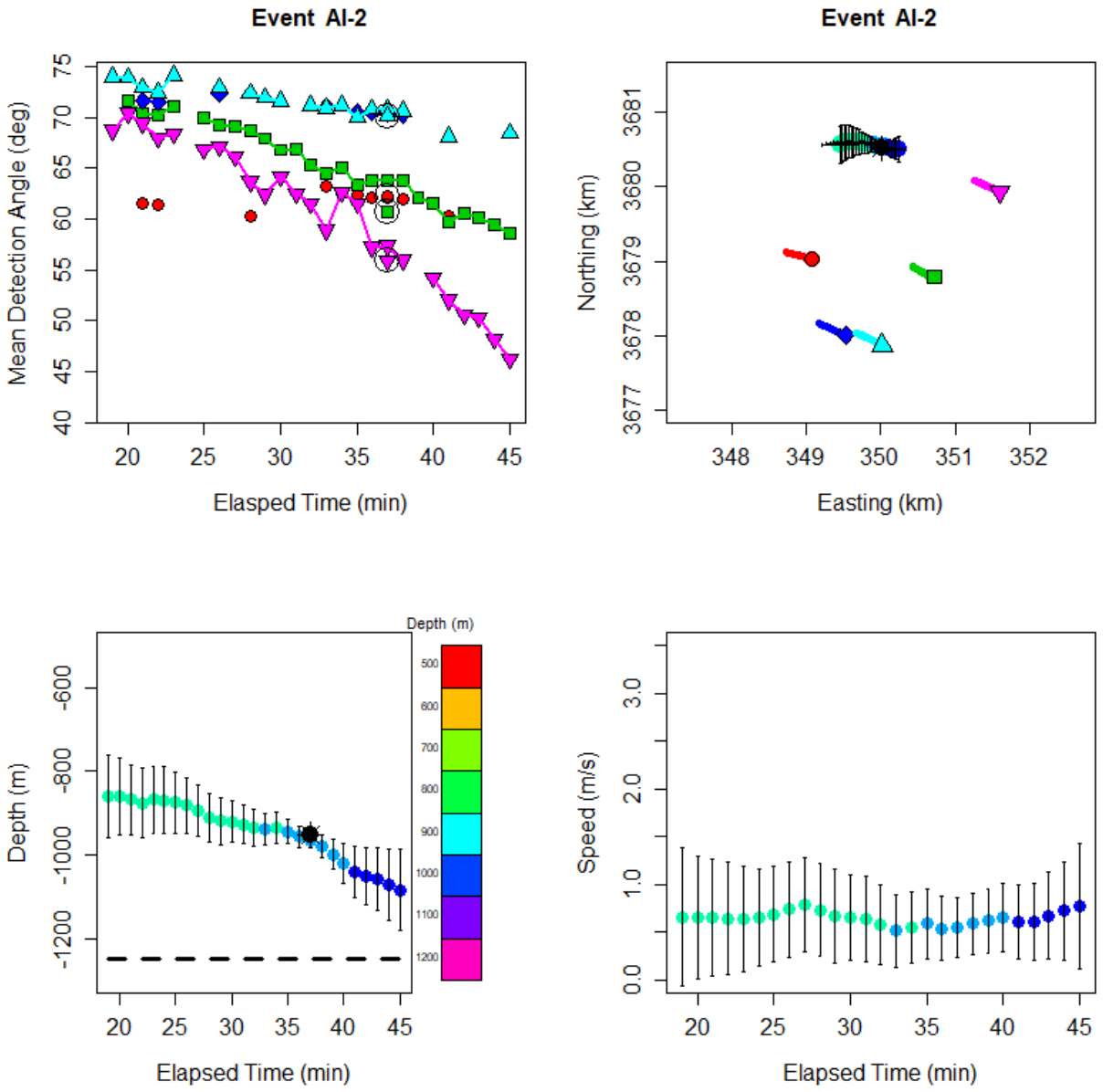

Supplementary Material 4. Additional figures.

FIG. S4. Detection angle data, estimated location track, estimated depth and estimated speed through the water for track AI-3. See figure captions for Fig. 2, 3, 5, and S1 for detailed explanation of each panel. Error bars are two standard deviations in the posterior distribution.

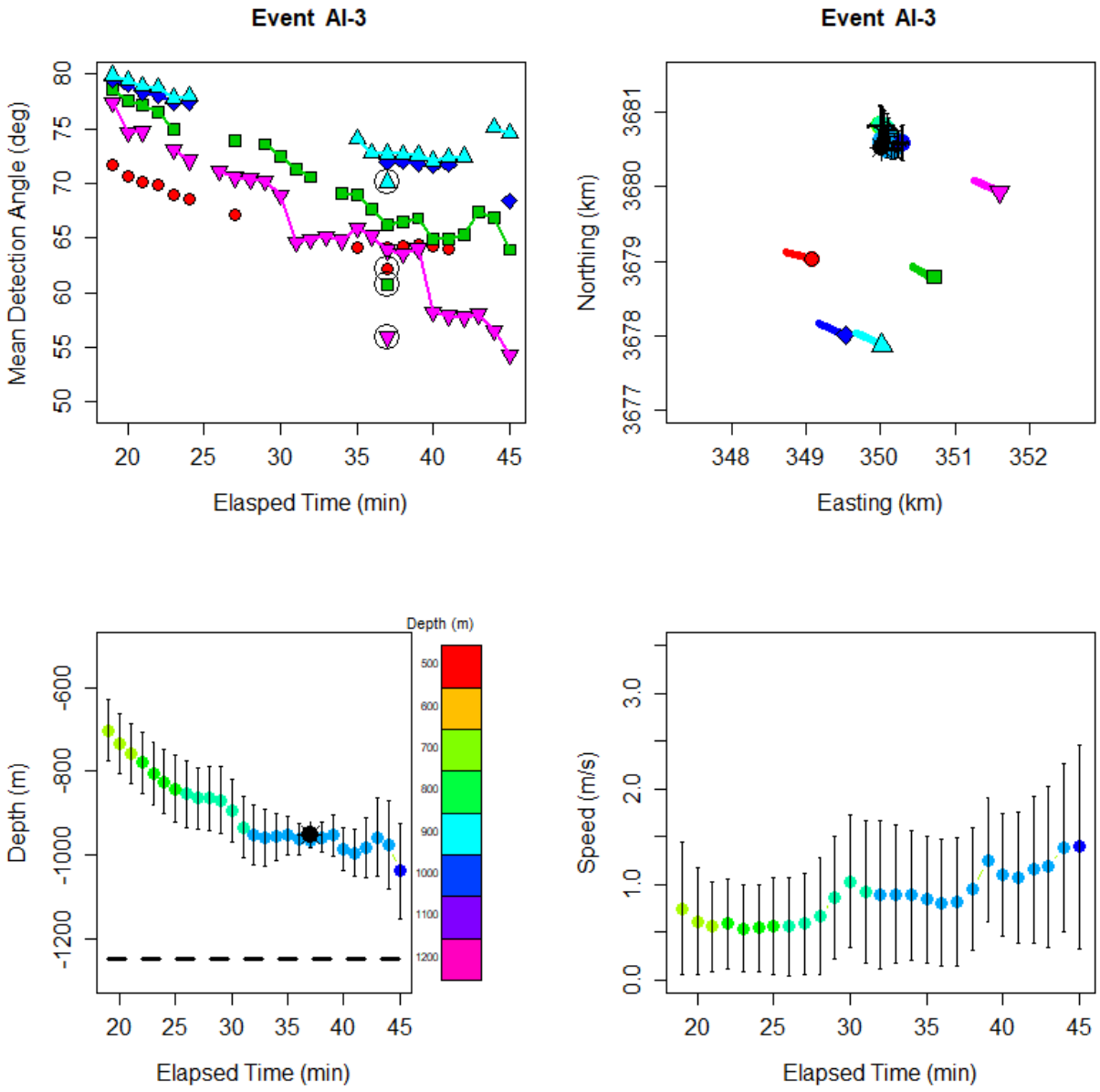

Supplementary Material 4. Additional figures.

FIG. S5. Detection angle data, estimated location track, estimated depth and estimated speed through the water for track AP-1. See figure captions for Fig. 2, 3, 5, and S1 for detailed explanation of each panel. Error bars are two standard deviations in the posterior distribution.

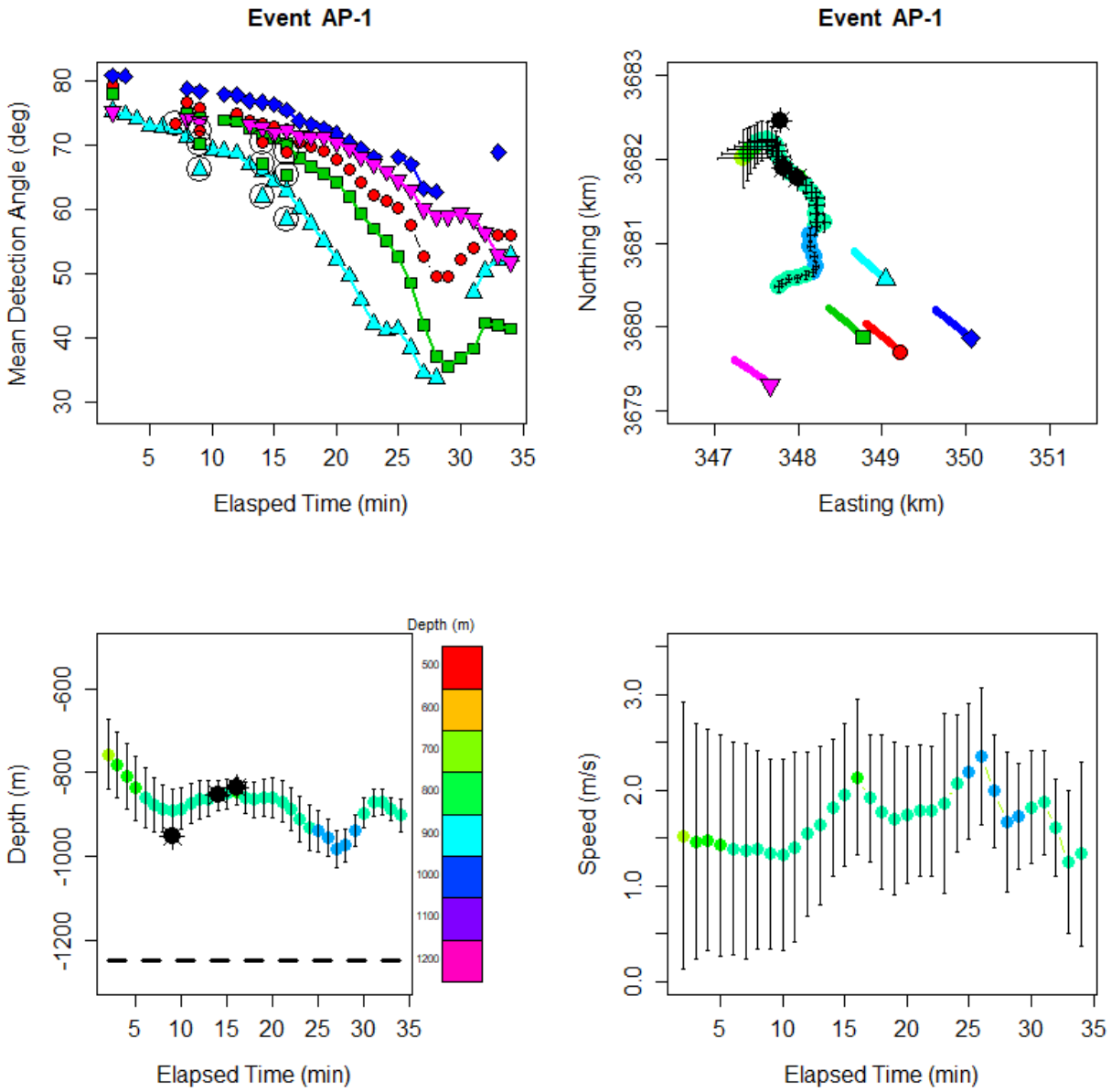

Supplementary Material 4. Additional figures.

FIG. S6. Detection angle data, estimated location track, estimated depth and estimated speed through the water for track AR-1. See figure captions for Fig. 2, 3, 5, and S1 for detailed explanation of each panel. Error bars are two standard deviations in the posterior distribution.

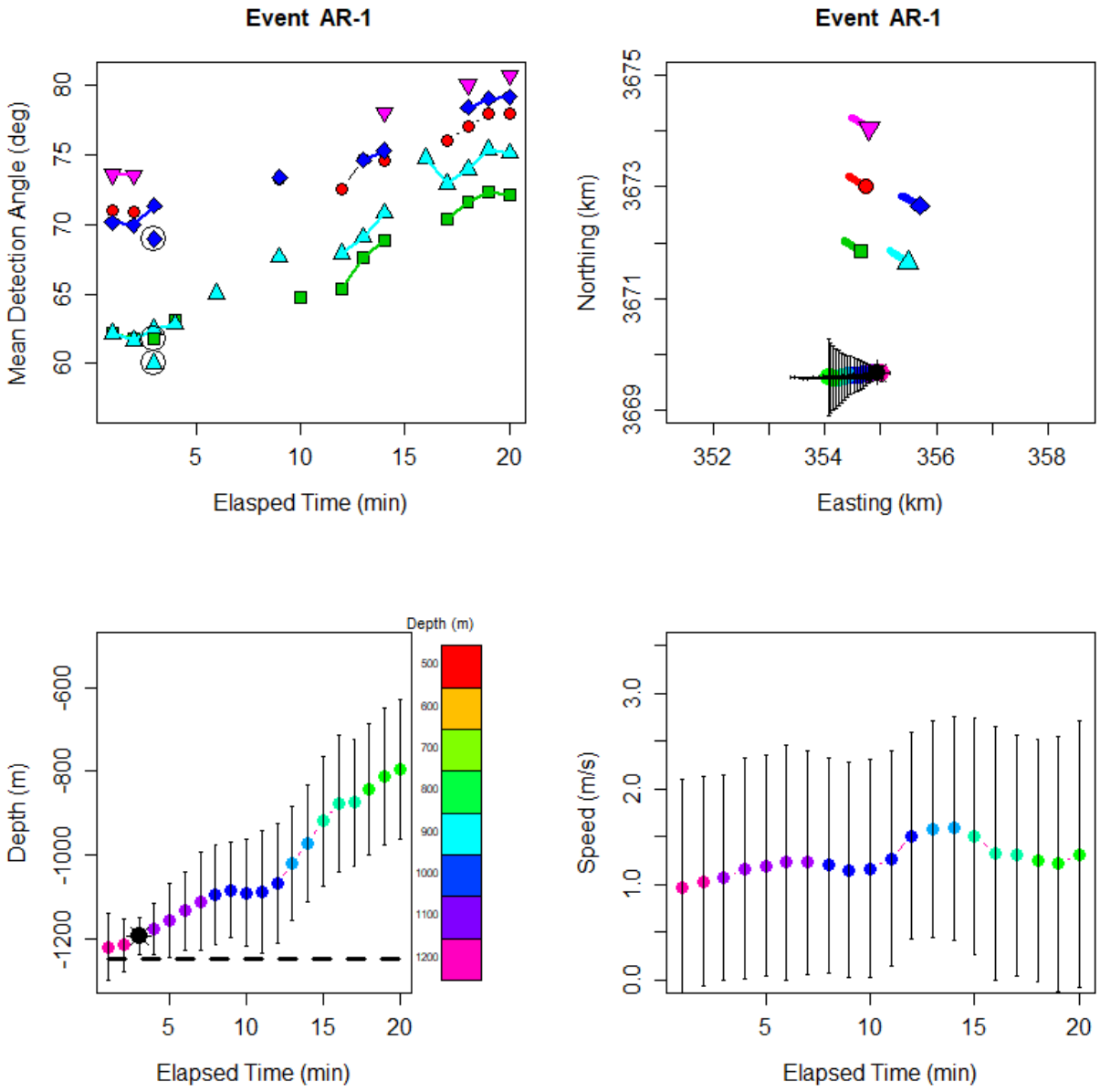

Supplementary Material 4. Additional figures.

FIG. S7. Detection angle data, estimated location track, estimated depth and estimated speed through the water for track AS-1. See figure captions for Fig. 2, 3, 5, and S1 for detailed explanation of each panel. Error bars are two standard deviations in the posterior distribution.

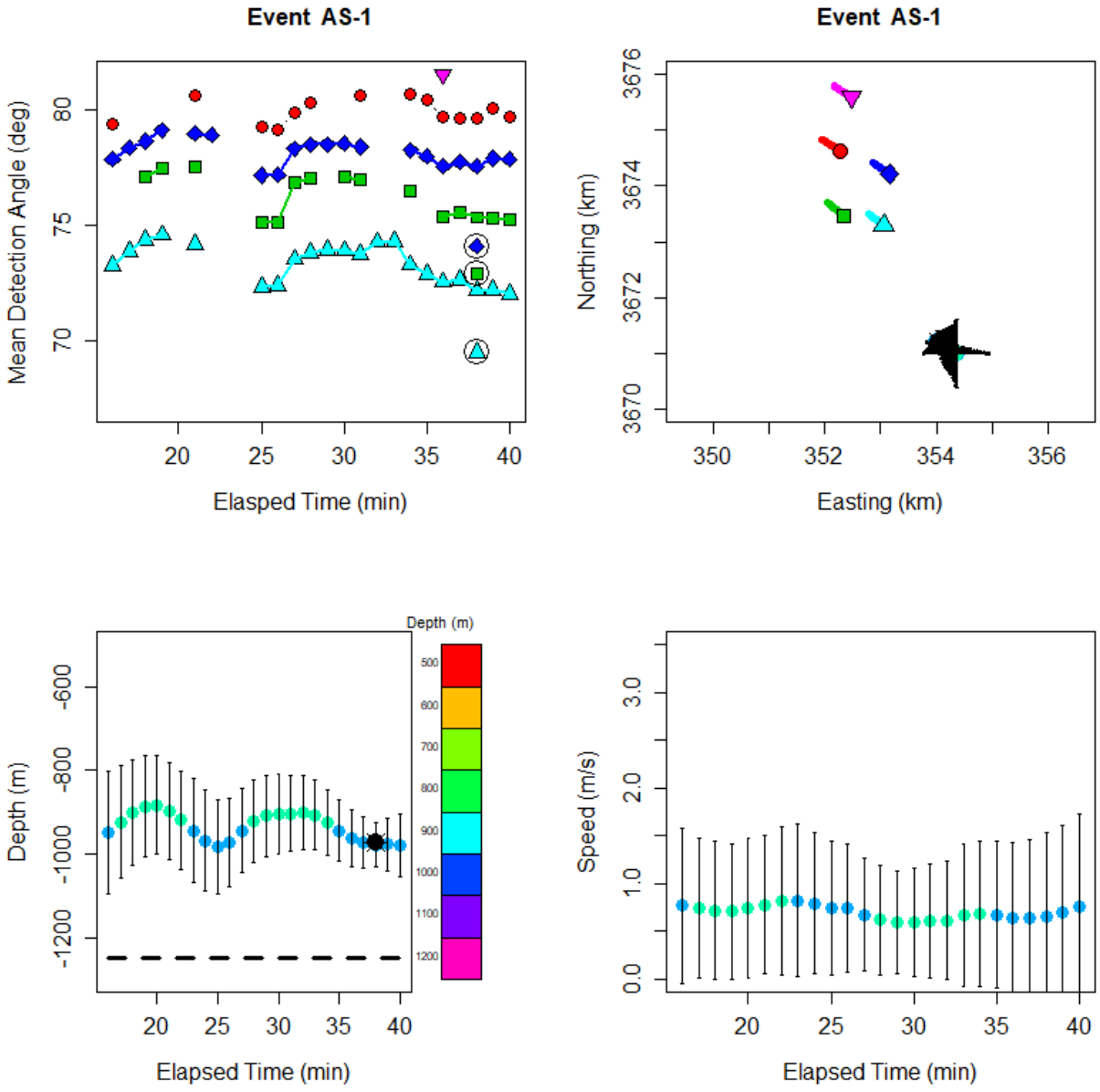

Supplementary Material 4. Additional figures.

FIG. S8. Detection angle data, estimated location track, estimated depth and estimated speed through the water for track AW-1. See figure captions for Fig. 2, 3, 5, and S1 for detailed explanation of each panel. Error bars are two standard deviations in the posterior distribution.

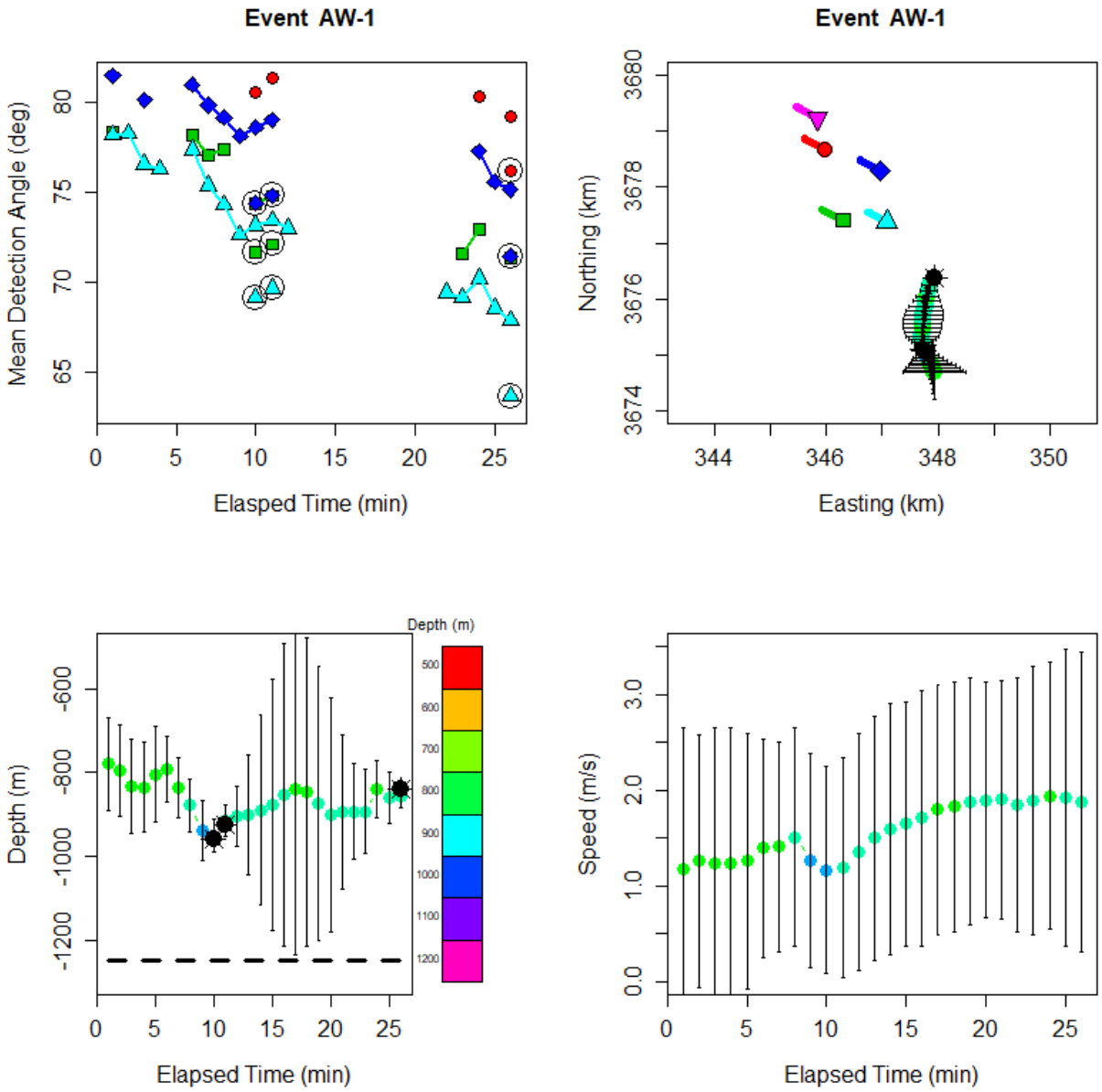

Supplementary Material 4. Additional figures.

FIG. S9. Detection angle data, estimated location track, estimated depth and estimated speed through the water for track BH-1. See figure captions for Fig. 2, 3, 5, and S1 for detailed explanation of each panel. Error bars are two standard deviations in the posterior distribution.

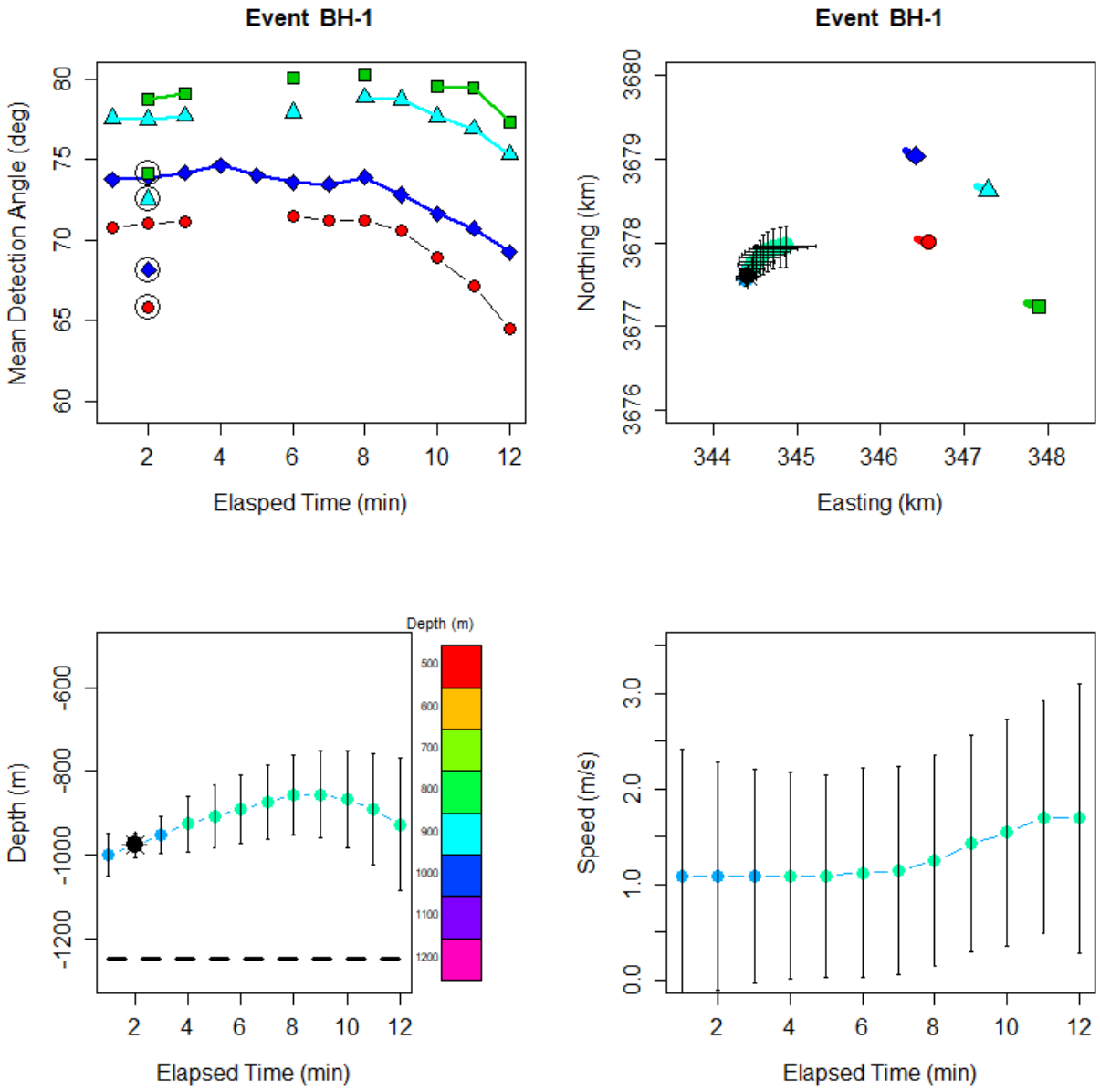

Supplementary Material 4. Additional figures.

FIG. S10. Detection angle data, estimated location track, estimated depth and estimated speed through the water for track BL-1. See figure captions for Fig. 2, 3, 5, and S1 for detailed explanation of each panel. Error bars are two standard deviations in the posterior distribution.

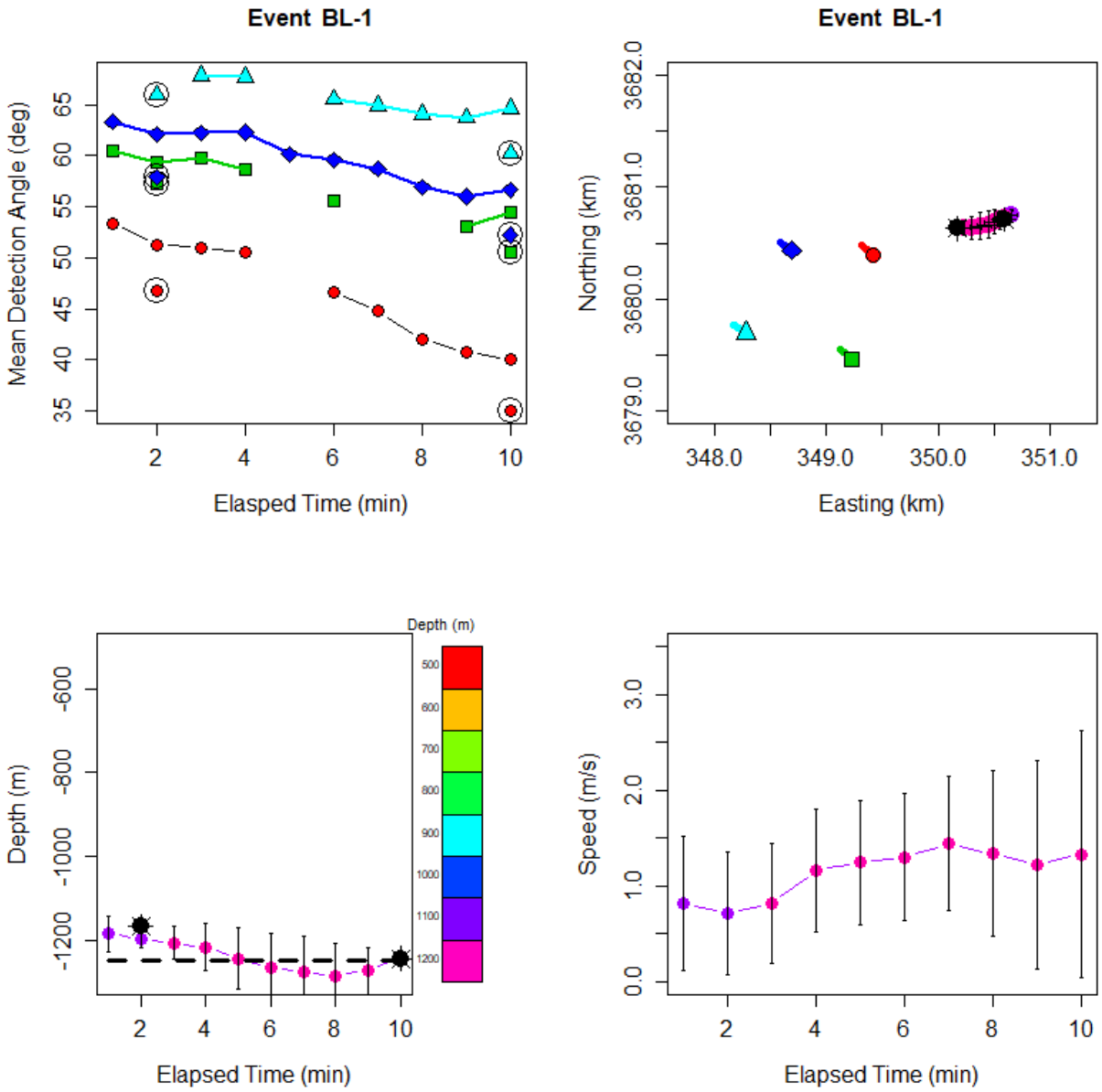

Supplementary Material 4. Additional figures.

FIG. S11. Detection angle data, estimated location track, estimated depth and estimated speed through the water for track BS-1. See figure captions for Fig. 2, 3, 5, and S1 for detailed explanation of each panel. Error bars are two standard deviations in the posterior distribution.

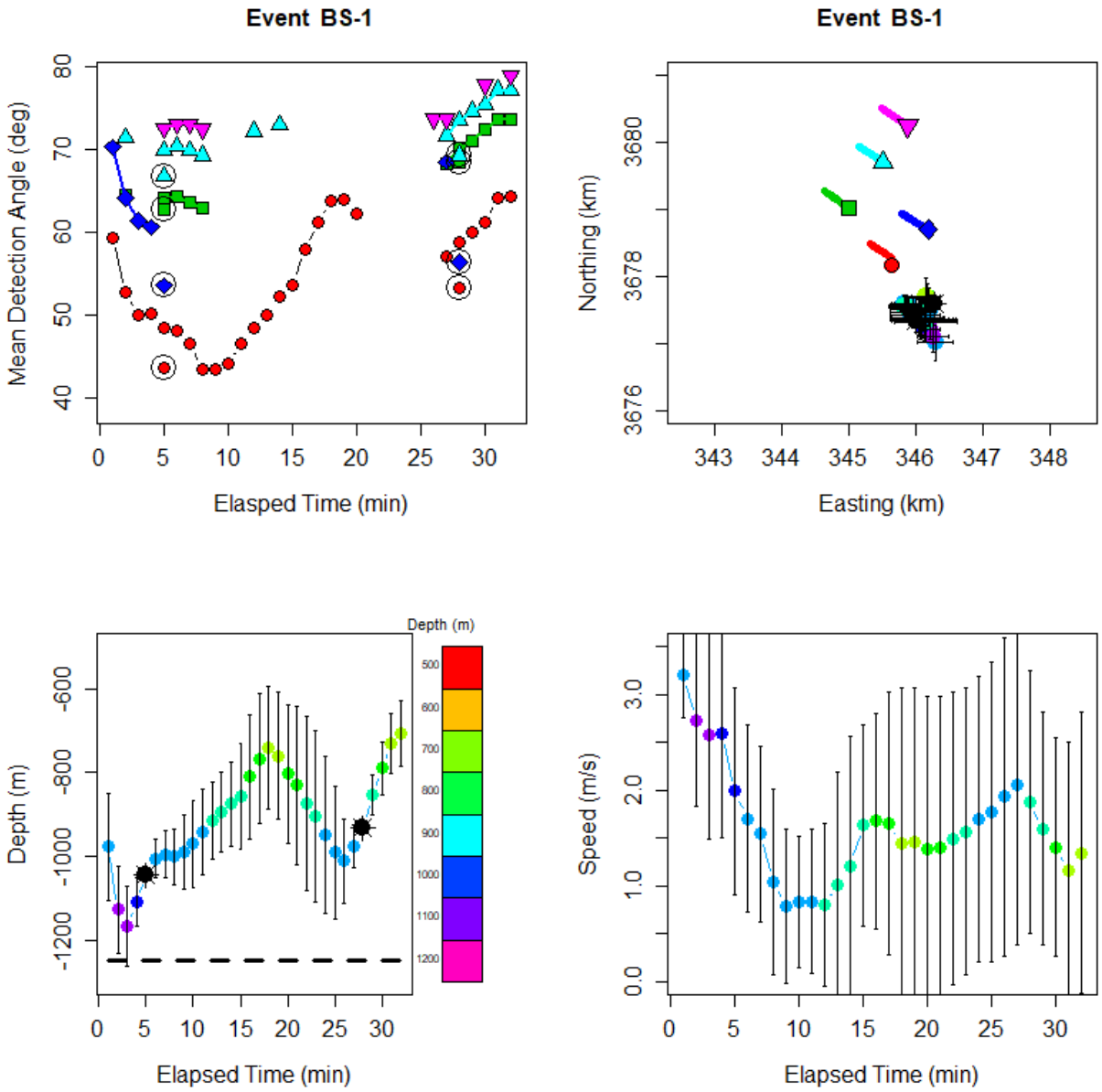

Supplementary Material 5. Track location output.

Table S2. Estimated 3D location for each minute of ten dive tracks. Easting and Northing are Universal Transverse Coordinates for Zone 11.

Dive Label	UTC Date & Time	Easting (Km)	Northing (Km)	Depth (Km)
AI-1	7/22/2016 3:48	349.050	3680.427	0.731
AI-1	7/22/2016 3:49	349.073	3680.445	0.769
AI-1	7/22/2016 3:50	349.095	3680.452	0.835
AI-1	7/22/2016 3:51	349.120	3680.457	0.901
AI-1	7/22/2016 3:52	349.143	3680.456	0.967
AI-1	7/22/2016 3:53	349.164	3680.451	1.032
AI-1	7/22/2016 3:54	349.184	3680.443	1.084
AI-1	7/22/2016 3:55	349.200	3680.436	1.125
AI-1	7/22/2016 3:56	349.212	3680.429	1.170
AI-1	7/22/2016 3:57	349.222	3680.420	1.215
AI-1	7/22/2016 3:58	349.233	3680.410	1.266
AI-1	7/22/2016 3:59	349.242	3680.394	1.323
AI-2	7/22/2016 4:06	349.449	3680.564	0.861
AI-2	7/22/2016 4:07	349.476	3680.577	0.859
AI-2	7/22/2016 4:08	349.506	3680.587	0.869
AI-2	7/22/2016 4:09	349.538	3680.596	0.876
AI-2	7/22/2016 4:10	349.568	3680.603	0.869
AI-2	7/22/2016 4:11	349.601	3680.607	0.870
AI-2	7/22/2016 4:12	349.634	3680.608	0.875
AI-2	7/22/2016 4:13	349.669	3680.606	0.882
AI-2	7/22/2016 4:14	349.706	3680.600	0.895
AI-2	7/22/2016 4:15	349.742	3680.592	0.912
AI-2	7/22/2016 4:16	349.781	3680.585	0.920
AI-2	7/22/2016 4:17	349.815	3680.578	0.921
AI-2	7/22/2016 4:18	349.849	3680.571	0.928
AI-2	7/22/2016 4:19	349.881	3680.564	0.936
AI-2	7/22/2016 4:20	349.912	3680.558	0.939
AI-2	7/22/2016 4:21	349.936	3680.554	0.935
AI-2	7/22/2016 4:22	349.963	3680.549	0.945
AI-2	7/22/2016 4:23	349.992	3680.545	0.957
AI-2	7/22/2016 4:24	350.019	3680.542	0.966
AI-2	7/22/2016 4:25	350.043	3680.536	0.980
AI-2	7/22/2016 4:26	350.066	3680.530	0.999
AI-2	7/22/2016 4:27	350.089	3680.523	1.020
AI-2	7/22/2016 4:28	350.116	3680.517	1.041
AI-2	7/22/2016 4:29	350.145	3680.515	1.051

AI-2	7/22/2016 4:30	350.174	3680.514	1.058
AI-2	7/22/2016 4:31	350.206	3680.512	1.071
AI-2	7/22/2016 4:32	350.240	3680.510	1.085
AI-3	7/22/2016 4:06	349.986	3680.816	0.703
AI-3	7/22/2016 4:07	349.989	3680.820	0.735
AI-3	7/22/2016 4:08	349.992	3680.823	0.759
AI-3	7/22/2016 4:09	349.997	3680.825	0.780
AI-3	7/22/2016 4:10	350.000	3680.824	0.806
AI-3	7/22/2016 4:11	350.002	3680.823	0.825
AI-3	7/22/2016 4:12	350.005	3680.824	0.842
AI-3	7/22/2016 4:13	350.011	3680.823	0.855
AI-3	7/22/2016 4:14	350.022	3680.821	0.865
AI-3	7/22/2016 4:15	350.038	3680.817	0.865
AI-3	7/22/2016 4:16	350.057	3680.805	0.869
AI-3	7/22/2016 4:17	350.079	3680.785	0.895
AI-3	7/22/2016 4:18	350.098	3680.756	0.934
AI-3	7/22/2016 4:19	350.094	3680.717	0.953
AI-3	7/22/2016 4:20	350.070	3680.681	0.960
AI-3	7/22/2016 4:21	350.041	3680.650	0.958
AI-3	7/22/2016 4:22	350.013	3680.617	0.954
AI-3	7/22/2016 4:23	350.005	3680.578	0.962
AI-3	7/22/2016 4:24	350.018	3680.541	0.966
AI-3	7/22/2016 4:25	350.043	3680.511	0.958
AI-3	7/22/2016 4:26	350.084	3680.492	0.954
AI-3	7/22/2016 4:27	350.142	3680.482	0.988
AI-3	7/22/2016 4:28	350.192	3680.500	0.997
AI-3	7/22/2016 4:29	350.224	3680.533	0.984
AI-3	7/22/2016 4:30	350.248	3680.572	0.959
AI-3	7/22/2016 4:31	350.282	3680.598	0.976
AI-3	7/22/2016 4:32	350.293	3680.592	1.040
AP-1	7/24/2016 6:09	347.347	3682.007	0.758
AP-1	7/24/2016 6:10	347.389	3682.062	0.783
AP-1	7/24/2016 6:11	347.429	3682.111	0.810
AP-1	7/24/2016 6:12	347.470	3682.152	0.838
AP-1	7/24/2016 6:13	347.504	3682.197	0.859
AP-1	7/24/2016 6:14	347.563	3682.219	0.878
AP-1	7/24/2016 6:15	347.625	3682.232	0.887
AP-1	7/24/2016 6:16	347.688	3682.210	0.892
AP-1	7/24/2016 6:17	347.725	3682.165	0.886
AP-1	7/24/2016 6:18	347.742	3682.106	0.875
AP-1	7/24/2016 6:19	347.761	3682.039	0.866
AP-1	7/24/2016 6:20	347.801	3681.968	0.863
AP-1	7/24/2016 6:21	347.842	3681.900	0.857

AP-1	7/24/2016 6:22	347.914	3681.831	0.852
AP-1	7/24/2016 6:23	348.007	3681.783	0.845
AP-1	7/24/2016 6:24	348.082	3681.690	0.862
AP-1	7/24/2016 6:25	348.152	3681.613	0.865
AP-1	7/24/2016 6:26	348.205	3681.536	0.861
AP-1	7/24/2016 6:27	348.222	3681.447	0.862
AP-1	7/24/2016 6:28	348.213	3681.351	0.870
AP-1	7/24/2016 6:29	348.219	3681.255	0.888
AP-1	7/24/2016 6:30	348.302	3681.239	0.912
AP-1	7/24/2016 6:31	348.216	3681.189	0.932
AP-1	7/24/2016 6:32	348.145	3681.092	0.941
AP-1	7/24/2016 6:33	348.144	3680.965	0.955
AP-1	7/24/2016 6:34	348.184	3680.836	0.984
AP-1	7/24/2016 6:35	348.211	3680.723	0.975
AP-1	7/24/2016 6:36	348.171	3680.644	0.939
AP-1	7/24/2016 6:37	348.084	3680.616	0.898
AP-1	7/24/2016 6:38	347.988	3680.579	0.873
AP-1	7/24/2016 6:39	347.879	3680.574	0.870
AP-1	7/24/2016 6:40	347.807	3680.519	0.888
AP-1	7/24/2016 6:41	347.762	3680.476	0.903
AR-1	7/24/2016 20:28	355.019	3669.651	1.222
AR-1	7/24/2016 20:29	354.979	3669.659	1.216
AR-1	7/24/2016 20:30	354.936	3669.661	1.196
AR-1	7/24/2016 20:31	354.889	3669.659	1.178
AR-1	7/24/2016 20:32	354.838	3669.653	1.158
AR-1	7/24/2016 20:33	354.785	3669.644	1.135
AR-1	7/24/2016 20:34	354.732	3669.634	1.112
AR-1	7/24/2016 20:35	354.676	3669.625	1.095
AR-1	7/24/2016 20:36	354.621	3669.620	1.085
AR-1	7/24/2016 20:37	354.569	3669.621	1.091
AR-1	7/24/2016 20:38	354.516	3669.621	1.089
AR-1	7/24/2016 20:39	354.460	3669.616	1.069
AR-1	7/24/2016 20:40	354.404	3669.602	1.021
AR-1	7/24/2016 20:41	354.347	3669.585	0.972
AR-1	7/24/2016 20:42	354.292	3669.572	0.920
AR-1	7/24/2016 20:43	354.236	3669.567	0.876
AR-1	7/24/2016 20:44	354.187	3669.570	0.875
AR-1	7/24/2016 20:45	354.141	3669.571	0.843
AR-1	7/24/2016 20:46	354.099	3669.574	0.813
AR-1	7/24/2016 20:47	354.061	3669.580	0.796
AS-1	7/24/2016 23:21	354.360	3670.986	0.951
AS-1	7/24/2016 23:22	354.353	3670.991	0.925
AS-1	7/24/2016 23:23	354.345	3670.996	0.902

AS-1	7/24/2016 23:24	354.335	3671.002	0.887
AS-1	7/24/2016 23:25	354.322	3671.011	0.883
AS-1	7/24/2016 23:26	354.306	3671.021	0.897
AS-1	7/24/2016 23:27	354.290	3671.032	0.919
AS-1	7/24/2016 23:28	354.272	3671.044	0.945
AS-1	7/24/2016 23:29	354.252	3671.057	0.968
AS-1	7/24/2016 23:30	354.232	3671.068	0.984
AS-1	7/24/2016 23:31	354.214	3671.076	0.973
AS-1	7/24/2016 23:32	354.202	3671.078	0.945
AS-1	7/24/2016 23:33	354.190	3671.083	0.922
AS-1	7/24/2016 23:34	354.176	3671.090	0.910
AS-1	7/24/2016 23:35	354.162	3671.098	0.905
AS-1	7/24/2016 23:36	354.147	3671.107	0.904
AS-1	7/24/2016 23:37	354.131	3671.116	0.901
AS-1	7/24/2016 23:38	354.115	3671.126	0.908
AS-1	7/24/2016 23:39	354.100	3671.138	0.925
AS-1	7/24/2016 23:40	354.084	3671.150	0.945
AS-1	7/24/2016 23:41	354.070	3671.161	0.963
AS-1	7/24/2016 23:42	354.056	3671.171	0.972
AS-1	7/24/2016 23:43	354.041	3671.180	0.978
AS-1	7/24/2016 23:44	354.027	3671.188	0.978
AS-1	7/24/2016 23:45	354.014	3671.196	0.980
AW-1	7/25/2016 7:45	347.936	3674.688	0.780
AW-1	7/25/2016 7:46	347.919	3674.725	0.795
AW-1	7/25/2016 7:47	347.905	3674.763	0.834
AW-1	7/25/2016 7:48	347.886	3674.809	0.835
AW-1	7/25/2016 7:49	347.870	3674.849	0.805
AW-1	7/25/2016 7:50	347.850	3674.894	0.793
AW-1	7/25/2016 7:51	347.828	3674.940	0.838
AW-1	7/25/2016 7:52	347.804	3674.986	0.879
AW-1	7/25/2016 7:53	347.784	3675.029	0.940
AW-1	7/25/2016 7:54	347.763	3675.077	0.952
AW-1	7/25/2016 7:55	347.747	3675.118	0.917
AW-1	7/25/2016 7:56	347.734	3675.168	0.905
AW-1	7/25/2016 7:57	347.723	3675.218	0.903
AW-1	7/25/2016 7:58	347.717	3675.274	0.890
AW-1	7/25/2016 7:59	347.716	3675.336	0.878
AW-1	7/25/2016 8:00	347.718	3675.404	0.855
AW-1	7/25/2016 8:01	347.721	3675.481	0.842
AW-1	7/25/2016 8:02	347.725	3675.558	0.847
AW-1	7/25/2016 8:03	347.734	3675.637	0.874
AW-1	7/25/2016 8:04	347.742	3675.717	0.901

AW-1	7/25/2016 8:05	347.753	3675.793	0.895
AW-1	7/25/2016 8:06	347.769	3675.869	0.893
AW-1	7/25/2016 8:07	347.790	3675.961	0.893
AW-1	7/25/2016 8:08	347.811	3676.044	0.841
AW-1	7/25/2016 8:09	347.833	3676.144	0.861
AW-1	7/25/2016 8:10	347.855	3676.242	0.858
BH-1	7/26/2016 9:18	344.387	3677.569	1.001
BH-1	7/26/2016 9:19	344.408	3677.609	0.978
BH-1	7/26/2016 9:20	344.430	3677.649	0.953
BH-1	7/26/2016 9:21	344.454	3677.690	0.927
BH-1	7/26/2016 9:22	344.483	3677.733	0.908
BH-1	7/26/2016 9:23	344.516	3677.776	0.893
BH-1	7/26/2016 9:24	344.553	3677.818	0.875
BH-1	7/26/2016 9:25	344.596	3677.855	0.858
BH-1	7/26/2016 9:26	344.652	3677.890	0.856
BH-1	7/26/2016 9:27	344.720	3677.918	0.869
BH-1	7/26/2016 9:28	344.792	3677.937	0.891
BH-1	7/26/2016 9:29	344.865	3677.951	0.927
BL-1	7/27/2016 8:10	350.657	3680.746	1.185
BL-1	7/27/2016 8:11	350.625	3680.735	1.199
BL-1	7/27/2016 8:12	350.596	3680.723	1.207
BL-1	7/27/2016 8:13	350.561	3680.707	1.218
BL-1	7/27/2016 8:14	350.510	3680.686	1.245
BL-1	7/27/2016 8:15	350.450	3680.666	1.267
BL-1	7/27/2016 8:16	350.382	3680.649	1.278
BL-1	7/27/2016 8:17	350.304	3680.638	1.286
BL-1	7/27/2016 8:18	350.232	3680.632	1.274
BL-1	7/27/2016 8:19	350.177	3680.630	1.243
BS-1	7/29/2016 12:40	346.290	3677.011	0.978
BS-1	7/29/2016 12:41	346.255	3677.099	1.128
BS-1	7/29/2016 12:42	346.207	3677.212	1.168
BS-1	7/29/2016 12:43	346.115	3677.281	1.110
BS-1	7/29/2016 12:44	345.997	3677.332	1.043
BS-1	7/29/2016 12:45	345.945	3677.409	1.007
BS-1	7/29/2016 12:46	345.923	3677.493	0.995
BS-1	7/29/2016 12:47	345.892	3677.567	1.001
BS-1	7/29/2016 12:48	345.860	3677.595	0.990
BS-1	7/29/2016 12:49	345.834	3677.595	0.971
BS-1	7/29/2016 12:50	345.824	3677.576	0.943
BS-1	7/29/2016 12:51	345.827	3677.558	0.915
BS-1	7/29/2016 12:52	345.842	3677.542	0.895
BS-1	7/29/2016 12:53	345.869	3677.526	0.876
BS-1	7/29/2016 12:54	345.906	3677.504	0.856

BS-1	7/29/2016 12:55	345.949	3677.465	0.811
BS-1	7/29/2016 12:56	345.993	3677.419	0.767
BS-1	7/29/2016 12:57	346.034	3677.381	0.741
BS-1	7/29/2016 12:58	346.063	3677.370	0.761
BS-1	7/29/2016 12:59	346.088	3677.370	0.804
BS-1	7/29/2016 13:00	346.120	3677.352	0.832
BS-1	7/29/2016 13:01	346.134	3677.337	0.874
BS-1	7/29/2016 13:02	346.143	3677.321	0.906
BS-1	7/29/2016 13:03	346.129	3677.339	0.949
BS-1	7/29/2016 13:04	346.130	3677.378	0.991
BS-1	7/29/2016 13:05	346.154	3677.431	1.012
BS-1	7/29/2016 13:06	346.206	3677.483	0.977
BS-1	7/29/2016 13:07	346.242	3677.575	0.930
BS-1	7/29/2016 13:08	346.218	3677.635	0.855
BS-1	7/29/2016 13:09	346.187	3677.670	0.790
BS-1	7/29/2016 13:10	346.168	3677.686	0.732
BS-1	7/29/2016 13:11	346.145	3677.704	0.708